

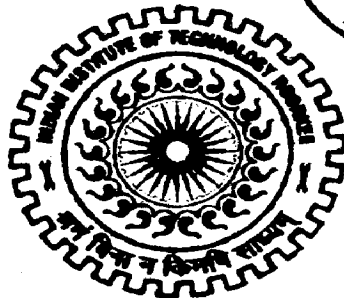
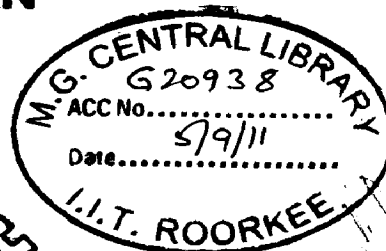
ROBUST LONG RANGE TARGET DETECTION ALGORITHM FOR AIRBORNE APPLICATIONS

A DISSERTATION

*Submitted in partial fulfillment of the
requirements for the award of the degree
of*
MASTER OF TECHNOLOGY
in
INFORMATION TECHNOLOGY

By

RAM SARAN



DEPARTMENT OF ELECTRONICS AND COMPUTER ENGINEERING
INDIAN INSTITUTE OF TECHNOLOGY ROORKEE
ROORKEE -247 667 (INDIA)
JUNE, 2011

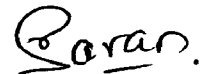
DECLARATION

I hereby declare that the work being presented in the dissertation report titled “**Robust Long Range Target Detection Algorithm for Airborne Applications**” in partial fulfillment of the requirement for the award of the degree of Master of Technology in Information Technology, submitted in the Department of Electronics and Computer Engineering, Indian Institute of Technology Roorkee, is an authentic record of my own work carried out under the guidance of Dr. Anil K. Sarje, Professor, Department of Electronics and Computer Engineering, Indian Institute of Technology Roorkee.

I have not submitted the matter embodied in this dissertation report for the award of any other degree.

Dated : 17 June 2011

Place : IIT Roorkee



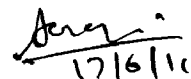
Ram Saran

CERTIFICATE

This is to certify that declaration made by the candidate is correct to the best of my knowledge and belief.

Dated : June 2011

Place : IIT Roorkee



Dr. Anil K. Sarje

Professor

Department of Electronics and Computer Engineering

ACKNOWLEDEMENT

First of all and foremost, I would like to express my deep sense of gratitude and indebtedness to my guide Dr. Anil K. Sarje, Professor, Department of Electronics and Computer Engineering for his invaluable guidance and constant encouragement throughout the dissertation.

I am also grateful to Dr. R. C. Joshi, Professor for his suggestions given during mid-term evaluation to further improve the results.

I would like to acknowledge Shri S. S. Sundaram, Distinguished Scientist and Director, IRDE, DRDO, Ministry of Defence, Dehradun for permitting me to carry out the part of my dissertation at IRDE.

My special acknowledgement to Shri H. B. Srivastava, Scientist 'G' and Associate Director, IRDE, Dehradun for his "taken for granted" help and support on technical as well as trivial matters, without which I am sure, my work, might have hit a dead end.

Last but not least, I would like to acknowledge my mother, my wife and my lovely daughter, Arunima who always encouraged and supported me during the carry out of my dissertation work and preparation of report.

Ram Saran

ABSTRACT

Early detection of air threats like aircrafts and missiles is becoming more and more important for advancing attack distance and response speed of modern hi-tech weapons in defence applications. These targets at longer ranges, typically 70 km or more, appear as point or small targets in visible and infrared image sequences. Because of the lack of apriori information about target dynamics and structural information such as shape, the detection of such targets becomes extremely challenging.

Recently many algorithms for detection of point and small targets for airborne applications have been reported in the literature. It is found that most of these algorithms are unable to adapt their behaviour to perform robustly in the rapidly changing environment. In addition, the high computational complexity of reported detection algorithms requires large processing hardware and leaves a little scope for real time implementation. Hence, a novel and robust long range target detection algorithm based on Adaptive Selective Double Structuring element Top-Hat Transform (Adapt-Sel-DSTHT) and maximum entropy criterion is proposed in this dissertation report. Experimental results show high probability of detection and low false alarms even for highly clouded scenario.

The proposed robust long range target detection algorithm has also been implemented on PowerPC hardware. AltiVec vector processing unit of PowerPC G4 is used to speed up the processing and lead to real-time detection of targets.

LIST OF FIGURES

| | |
|--|----|
| Figure 1.1 : IRST System Configuration..... | 2 |
| Figure 1.2 : Block Diagram of IRST Algorithms..... | 3 |
| Figure 3.1 : Block Diagram of Proposed Robust Target Detection Algorithm..... | 14 |
| Figure 3.2 : Flow Diagram of Proposed Robust Target Detection Algorithm..... | 18 |
| Figure 4.1 : Snapshot of the GUI of the ALoRT-DetSys..... | 20 |
| Figure 4.2 : Snapshot of the GUI of the ALoRT-DetSys during Offline Processing.. | 21 |
| Figure 4.3 : Simulation Setup of the ALoRT-DetSys for Online Processing..... | 21 |
| Figure 4.4 : Snapshot of the GUI of the ALoRT-DetSys during Online Processing.. | 22 |
| Figure 4.5 : Pre-Processing Result-1..... | 23 |
| Figure 4.6 : Pre-Processing Result-2..... | 24 |
| Figure 4.7 : Pre-Processing Result-3..... | 25 |
| Figure 4.8 : Pre-Processing Result-4..... | 26 |
| Figure 4.9 : Pre-Processing Result-5..... | 27 |
| Figure 4.10: Plot of MARB..... | 28 |
| Figure 4.11: Detection Results-1..... | 30 |
| Figure 4.12: Detection Results-2..... | 31 |
| Figure 4.13: Detection Results-3..... | 32 |
| Figure 4.14: Detection Results-4..... | 33 |
| Figure 4.15: Detection Results-5..... | 34 |
| Figure 4.16: Detection Result for Extended Size Targets (3x3 Pixels)..... | 35 |
| Figure 4.17: Detection Result for Extended Size Targets (5x5 Pixels)..... | 36 |
| Figure 5.1 : VME Chassis..... | 38 |
| Figure 5.2 : SVME 183 PowerPC Board..... | 39 |
| Figure 5.3 : PMC 704 Graphics Input/Output Card..... | 39 |
| Figure 5.4 : Camera Mounted on Scanning Gimbal..... | 39 |
| Figure 5.5 : SVME-183 Core Processing Architecture..... | 41 |
| Figure 5.6 : Execution Units of PowerPC G4..... | 41 |
| Figure 5.7 : Scalar and Vector Processing..... | 42 |
| Figure 5.8 : Organization of Image for Vectorized Morphological Processing..... | 44 |
| Figure 5.9 : Snapshot of Display/ Overlaying Output..... | 47 |
| Figure 5.10: Hardware Implementation Results..... | 49 |
| Figure 5.11: Components of Hardware Implementation..... | 50 |
| Figure 5.12: Laboratory Prototype..... | 50 |

LIST OF TABLES

| | |
|--|----|
| Table 4.1: Probability of Detection and Probability of Probability of False Alarm..... | 37 |
| Table 5.1: Run-Time for Hardware Implementation of Gray-Scale Morphological Processing Algorithm..... | 46 |

TABLE OF CONTENTS

| | | |
|----------|--|------------|
| | <i>Declaration and Certificate</i> | <i>i</i> |
| | <i>Acknowledgement</i> | <i>ii</i> |
| | <i>Abstract</i> | <i>iii</i> |
| | <i>List of Figures</i> | <i>iv</i> |
| | <i>List of Tables</i> | <i>v</i> |
| 1 | Chapter 1. Introduction | 1 |
| | 1.1 Infra-Red Search and Track (IRST) Systems | 1 |
| | 1.2 Long Range Target Detection Algorithms..... | 2 |
| | 1.3 Problem Statement | 4 |
| | 1.4 Organization of Report | 4 |
| 2 | Chapter 2. Literature Review | 5 |
| | 2.1 Pre-Processing Algorithms..... | 6 |
| | 2.2 Detection Algorithms | 8 |
| 3 | Chapter 3. Proposed Robust Long Range Target Detection Algorithm | 14 |
| | 3.1 Pre-Processing Algorithm..... | 14 |
| | 3.2 Detection Algorithm..... | 15 |
| | 3.3 Performance Measures | 16 |
| 4 | Chapter 4. Simulation Methodolgy and Results | 19 |
| | 4.1 Graphical User Interface Design | 19 |
| | 4.2 Simulation Setup..... | 21 |
| | 4.3 Results and Performance Comparisons | 22 |
| 5 | Chapter 5. Real-Time Implimentation on PowerPC Hardware | 38 |
| | 5.1 Hardwares and Softwares Used for Hardware Implementation | 38 |
| | 5.2 Overview of PowerPC (AltiVec)..... | 41 |
| | 5.3 Real-Time Implimentation of Morphological Pre-Processing Algorithm Using AltiVec..... | 42 |

| | |
|--|------------------|
| 5.4 Real-Time Implementation of Robust Long Range Target Detection | |
| Algorithm | 46 |
| 5.5 Real-Time Video Capture, Display and Overlaying Module | 47 |
| 5.6 Hardware Implementation Results..... | 48 |
| 5.7 Laboratory Prototype and Experimental Setup | 50 |
| 6 Chapter 6. Conclusion and Future Scope..... | 51 |
| <i>Research Publications and Award.....</i> | <i>52</i> |
| <i>References.....</i> | <i>53</i> |

1 INTRODUCTION

Early detection of air threats like aircrafts and missiles is becoming more and more important for advancing attack distance and response of modern weapons in defence applications. To encounter this problem, airborne Infra-Red Search and Track (IRST) systems [1-2] are required for fighter aircrafts to enable them to passively search, detect, track, classify and prioritize multiple incoming intruder aircrafts and engage them at as long ranges as possible. While the IRST systems have been proven in performance for ground-based and naval-based platforms, but these are still facing some technical problems for airborne applications. These problems arise from uncertainty in target signature, atmospheric effects, background clutter (especially dense and varying clouds), signal and image processing algorithms to detect potential targets at long ranges as well as some hardware limitations such as large memory requirement to store and process wide field of view data in real time.

1.1 INFRA-RED SEARCH AND TRACK (IRST) SYSTEMS

IRST systems are becoming of more and more important in air defence applications due to increased reluctance to use Radar sensors because of threat of anti radiation missiles and dramatic increase in infra-red (IR) sensor performance. On the other hand, targets are becoming less and less observable and the requirements are becoming more and more stringent for example, larger field of view, more dense and complex backgrounds with target entering from all directions with higher speeds and requirement to detect point and small targets at long ranges. In addition to that, IRST should be able to detect and track targets below the horizon and should provide landing and flying-aid capability in night and bad weather conditions. While operating with all above scenarios, the detection rate should be very high, typically >95%, and at the same time false alarm rate should be less than one per hour. The IRST system should be able to track single as well as multi targets. IRST system should also be able to give range information while target is beyond the scope of active range devices like laser range finder.

IRST system basically consists of a Sensor Head Unit (SHU) along with its control electronics and Signal Processing Unit (SPU). The Sensor Head Unit consists of a stabilized scanning mirror, an Infra-red (IR) sensor and a laser range finder (LRF). The scanning mirror scans the required field of view and project the radiated energy on to IR detector. The IR detector with its electronics forms the IR image and transfer to the SPU via high speed Low Voltage Differential Signaling (LVDS) link. The output of LRF and other commands are transferred between the head and the SPU. The Signal Processing Unit (SPU) implements the algorithms for detection and tracking of long range airborne targets. The target tracks information is send to the mission computer of aircraft via MIL STD 1553 avionics bus. The IRST system configuration is shown in Figure 1.1.

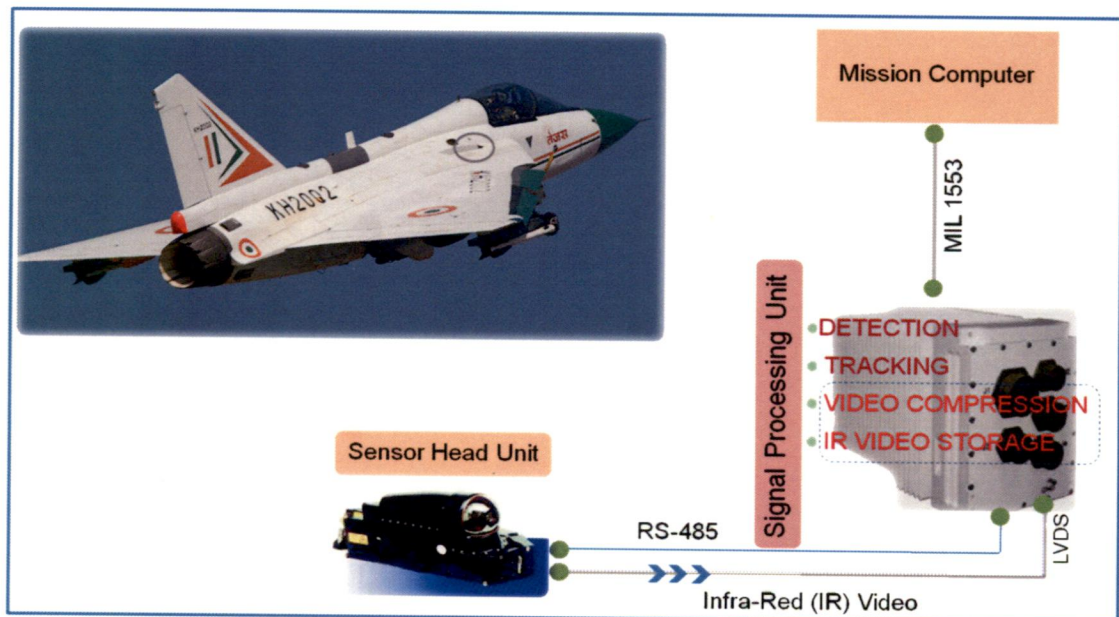


Figure 1.1: IRST System Configuration

1.2 LONG RANGE TARGET DETECTION ALGORITHMS

Airborne threats like aircrafts and missiles at longer ranges appear as point and small targets in visible and infrared image sequences. Because of the lack of apriori information about target dynamic and structural information such as shape, the detection of such targets becomes extremely challenging. Therefore, point and small target detection algorithms become crux of IRST system and play vital role in the success of such systems. Typically, the spatial pre-processing

step is performed on the input image to predict the background and consequently enhance the signal-to-clutter ratio. The detection algorithm may result in many false targets and this requires using the post processing algorithms [3-4] to reduce the false alarms. The block diagram of IRST algorithms is given in Figure 1.2.

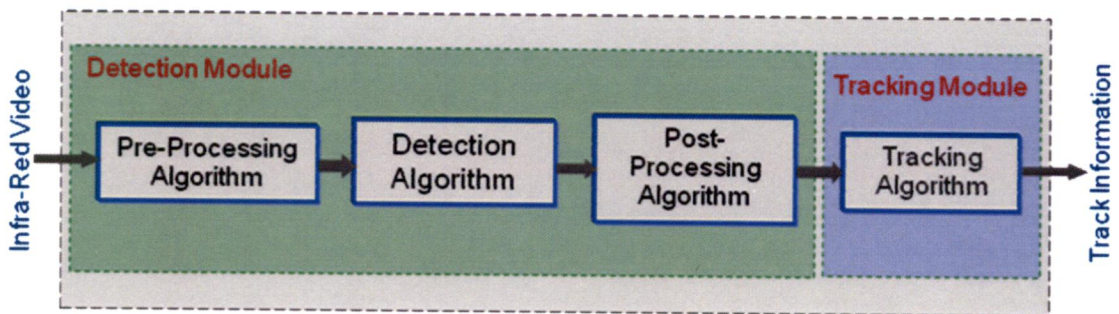


Figure 1.2: Block Diagram of IRST Algorithms

Real time detection of airborne targets in IR image sequences is a challenging task. Complex airborne application presents a number of operational requirements:

- Real-time detection and tracking capability.
- Wide-field-of-view results in large volume of data storage and processing requirement, hence complex electronics is required to implement the algorithms.
- Targets at long distances, when projected on the IR image plane /image sequence, appear as pixel/sub-pixel targets.
- Not only the target size grows or becomes smaller as the targets come close or recede away from sensor, the intensity level also undergoes variation depending on their aspect angles, atmospheric conditions, maneuver etc.
- Some of the targets may be pixel size, where as the others may be extended targets.
- Some of the targets may moving very slow, appearing as if they are static, while the others may be moving at great relative velocities.

1.3 PROBLEM STATEMENT

“To develop long range target detection algorithm for detection of low contrast, point or small airborne targets in Infra-Red (IR) image sequences of rapidly changing scenario to provide day-night early warning capability for fighter aircrafts”

1.4 ORGANIZATION OF REPORT

Chapter 2 gives a brief literature review of state-of-the-art point or small target detection algorithm for visible or IR image sequences.

Chapter 3 explains the proposed “Robust Long Range Target Detection Algorithm”. This chapter first describes the proposed “Adaptive Selective Double Structuring Element Top-Hat Transform (Adapt-Sel-DSTHT)” for effective clutter removal followed by proposed detection algorithm.

Chapter 4 presents the simulation methodology and results. The chapter also describes the GUI design and simulation setup.

Chapter 5 describes the real-time implementation of the proposed “Robust Long Range Target Detection Algorithm” on PowerPC hardware. The chapter also gives overview of PowerPC processor and explains the proposed “Vectorization of Constant-Time Gray-Scale Morphological Processing Algorithm Using AltiVec”. Hardware implementation results of the proposed “Robust Long Range Target Detection Algorithm” are also presented in this chapter.

Chapter 6 concludes the report and emphasizes the future scope.

2 LITERATURE REVIEW

Pre-Processing of incoming visible or IR image is a necessary step in the detection of airborne targets. A number of pre-processing algorithms have been suggested in literature like max-median [5], morphological filtering [6-9], top-hat transformation [10] and double window filtering (DWF) [11]. Max-median filter preserves the edges of clouds and structural background. But it removes low contrast point target also, which is a serious limitation. Mathematical morphology is widely used in the area of image processing as image filtering. Wavelet transform based detection algorithms [12-14], entropy based detection [6], motion analysis based detection [6], [15] and adaptive morphological clutter elimination [16] based detection have been published to detect small targets in dense clutter scenario. Temporal processing based on change detection [17] has also been published. A top-hat transform based small target detection algorithm [18] is published in the literature suitable for heavily cluttered scenario. The fusion-based algorithm [19] has also been reported in the literature which combines two independent detection algorithms to increase the detection rate. But all above reported methods suffer from one problem or the other and are suitable for a particular kind of scenario. For example, wavelet based detection algorithms high computation and data storage requirement which results in complex and large electronics.

Although target detection algorithms have been steadily improving, target detection systems are still only partially successful especially for airborne applications. Reported algorithms are often unable to detect targets reliably in the presence of highly cluttered scene. If they are able to detect then generates lots of false alarms and reducing the false alarms results in miss detection of true targets. In addition, all above reported algorithms are unable to adapt their behaviour to perform robustly in the rapidly changing environment. These reasons motivated to work on the development of robust long-range, point and small target detection algorithm for infra-red image sequences.

In addition to critical literature survey, state-of-the-art pre-processing algorithms and detection algorithms suitable for airborne applications have been implemented and their performance has been evaluated as part of this

dissertation work. Max-median filter, morphological filters and contour structuring element based top-hat transform have been implemented as pre-processing algorithms. Modified motion analysis (MMA) based target detection algorithm and adaptive morphological clutter elimination algorithm have been simulated for performance evaluation.

2.1 PRE-PROCESSING ALGORITHMS

Pre-Processing of incoming IR data is a necessary step in the detection of airborne targets. It has experimentally been verified that the detection of dim point size targets in cluttered background is not possible without increasing the SCR by pre-processing of IR data.

2.1.1 MAX-MEDIAN FILTER

Max-median filter preserves the edges of clouds and structural background. But it removes low contrast point target also, which is a serious limitation. In this filter, an NxN window is run over the image. The value of N, which is fixed, may be chosen as a tuning parameter (higher value results in higher complexity) to real situation demands. Median is found for column and row vector and two diagonal vectors with respect to center pixel of window. Next, the intensity value for the center pixel of the window is replaced by a maximum of these median values found. For max-median filters, with 3x3 pixels of window, $I(x, y)$ is replaced by a value as given by equation (2.1).

$$\begin{aligned}
 J(x,y) &= \max (med_1, med_2, med_3, med_4) \\
 \text{where } med_1 &= med(I(x,y-1), I(x,y), I(x,y+1)), \\
 med_2 &= med(I(x-1,y), I(x,y), I(x+1,y)), \\
 med_3 &= med(I(x-1,y-1), I(x,y), I(x+1,y+1)), \\
 med_4 &= med(I(x+1,y-1), I(x,y), I(x-1,y+1))
 \end{aligned} \tag{2.1}$$

where, $I(x, y)$ is the intensity of the pixel at row x and column y in the input image and $J(x, y)$ is the intensity of the pixel at row x and column y in the filtered image.

2.1.2 MORPHOLOGICAL FILTERS

Mathematical morphology is widely used in the area of image processing for image filtering. Gray-scale dilation and erosion are basic operations of mathematical morphology. Gray-scale opening and closing operations are

carried out with gray-scale dilation and erosion. The various morphological filters have been proposed and used [6]-[9] for background estimation.

Let $f(x, y)$ and $g(x, y)$ are input image and structuring element respectively. The gray scale dilation, erosion, opening and closing of f with structuring element g are defined by equations (2.2)-(2.5) respectively.

$$(f \oplus g)(s, t) = \max\{f(s-x, t-y) + g(x, y) \mid (s-x), (t-y) \in D_f; (x, y) \in D_g\} \quad (2.2)$$

$$(f \ominus g)(s, t) = \min\{f(s-x, t-y) - g(x, y) \mid (s-x), (t-y) \in D_f; (x, y) \in D_g\} \quad (2.3)$$

$$f \circ g = (f \ominus g) \oplus g \quad (2.4)$$

$$f \bullet g = (f \oplus g) \ominus g \quad (2.5)$$

The gray scale morphological top-hat transform of an image, denoted by T_f that enhances the target is defined by equation (2.6).

$$T_f = f - (f \circ g) \quad (2.6)$$

A hybrid filter also helps to enhance the target is defined as given by equation (2.7).

$$H_f = ((f \bullet g) + (f \circ g)) / 2 \quad (2.7)$$

The result of pre-processing depends on size and shape of structuring element. The usage of gray-scale morphological filtering is hampered due to its computation complexity. The performance of classical morphological filters discussed above become poor under highly clouded scenario and lead to higher false alarms by subsequent processing by detection algorithms.

2.1.3 CONTOUR STRUCTURING ELEMENT BASED TOP-HAT TRANSFORM

The small target embedded in the image acts as noise and the small target detection can be recognized as noise filtering, which is the base of small target detection by using mathematical morphology. But, because of the defect of image detail smoothing, the classical mathematical morphology based methods are inefficient if the clutter is heavy and the target is dim. To protect the image

details, some operations of contour structuring element based (CB) morphology has been reported in the literature [16].

Let f and g represent the grey-level image and a structuring element respectively, and ∂g be the contour of g following the connectivity of g . CB closing and CB white top-hat transform are defined by equations (2.8) and (2.9) respectively.

$$C_{CB} = (f \bullet \partial g) \circ g \quad (2.8)$$

$$WTH_{CB} = f - C_{CB} \quad (2.9)$$

2.2 DETECTION ALGORITHMS

2.2.1 MODIFIED MOTION ANALYSIS (MMA) BASED DETECTION ALGORITHM

The MMA based point target detection algorithm uses multi-frame processing and turns to temporal domain. The MMA based detection algorithm is able to detect point and/ extended target with very large target movement per image frame. In this algorithm, first input image frame is pre-processed by morphological filters. Conjunction function calculation is performed on each pixel of the image frame instead of only expected target pixels. This takes care of fast moving targets, targets with fast movement from frame to frame. Entropy information of the image sequence is also calculated in parallel and a threshold is established as a function of the entropy of image frame. This takes care of slow moving targets. Finally, the results of both approaches are combined. The MMA algorithm reported higher probability of detection but generates many false alarms for highly clouded background. The formal description of the MMA algorithm is given below.

Algorithm: MMA Algorithm

1. Perform gray-scale opening and closing operation on input image I_{seq} .
2. Calculate $J=Closing(Opening(I))$ and $K=Opening(Closing(I))$
3. Calculate $F=(J+K)/2$.
4. Calculate residue (difference) image, $D_{seq} = I_{seq} - F$.
5. Calculate entropy of the image frame and Calculate threshold for the image frame.
6. Perform thresholding on D_{seq} and get target output image O_1 .
7. Calculate conjunction function,
$$d_{seq}(i, j) = \min[c * (I_{seq}(i+n_i, j+n_j) - I_{seq-1}(i, j))]$$
where $n_i, n_j \in \sigma$ denote adjacent domain of some pixel, c is a constant
8. Perform thresholding operation, $|d_{seq}(i, j)| \leq \varepsilon$ and get target output image O_2 .
9. Combine outputs of step 7 and 8 by 'OR' ing operation.
10. Generate candidate target list.

2.2.2 ADAPTIVE MORPHOLOGICAL CLUTTER ELIMINATION (AMCE) BASED DETECTION ALGORITHM

Detection of dim small target in infrared or visible image sequences with heavy clutter is crucial for different image processing applications. The most pivotal counterpart of small target detection in heavy clutter image is to enhance the dim point target, by eliminating the clutter of the original image. So, accurate estimation of the clutter background is crucial for target detection. To overcome the affection of heavy clutter and dim target intensity in small target detection, an efficient morphological method for clutter elimination is proposed by Bai et al [16]. Based on CB morphology, a top-hat transformation is used and then modified to form an adaptive morphological method, which is used to enhance the small target through eliminating the clutter background of the small target image. This method imports the property of the target region into the morphological operations, which apparently improves the performance of the method and can largely enhance the dim small target. The Adaptive Morphological Clutter Elimination (AMCE) is used to suppress the clutter for enhancement of small targets. The resultant image after AMCE will contain large number of pixels with low gray values, and the histogram of the image will be uni-mode. So, it is not easy to find an appropriate threshold automatically. Fortunately, because of AMCE, the target is brighter than other regions in the result image of AMCE.

Then, the threshold can be obtained through the mean value and the maximum value of the result image of AMCE. The formal description of the MMA algorithm is given below.

Input: Image, IN

Output: Image, OUT

1. Compute $R = CBC_g(IN)$
2. Locate Window $w_{i,j}$ in IN and find $\max w_{i,j}$ and $\min w_{i,j}$ then Calculate,
3. Estimate the Background of the Image as:
If $I(i, j) - R(i, j) < T(w_{i,j})$, $BG(i, j) = I(i, j)$, else $BG(i, j) = R(i, j)$
4. Compute $CBWTH = IN - BG$
5. Calculate the Threshold Th as follows: $T(w_{i,j}) = \max w_{i,j} - \min w_{i,j}$
6. Calculate the maximum and mean grey scale values of image MCBTH as $\max V$ and $\text{mean} V$ respectively.
7. Calculate, $Th = \text{ratio} * \text{mean} V + (1 - \text{ratio}) * \max V$, where, $\text{ratio} = \text{mean} V / \max V$
8. Threshold image MCBTH with threshold value, Th and store result in image, OUT.

2.2.3 WAVELET BASED DETECTION ALGORITHM

Many small target detection algorithms based on wavelet analysis have been reported in literature [20-21]. The fundamental principle of wavelet transform is to decompose signals over dilated and translated wavelets. The fast calculating algorithm of Mallet's discrete dyadic wavelet transform point out that the image can be decomposed into four sub-images by using the low pass filter and high pass filter.

Due to the nice localization ability and directional characteristic of wavelet multi-resolution analysis, an effective target detection algorithm based on wavelet transform is reported in [20]. Firstly, the original image is decomposed twice by wavelet transform to get its horizontal and vertical high frequency image. Secondly, according to the certain selection criterion, the horizontal and vertical high frequency coefficients are preserved separately in the direction of column and row. Finally, infrared small target is detected by fusing the horizontal and vertical preserved results.

At a given level k , the signal C^k , called approximation signal, is split up into two terms [20]: a new approximation signal at a coarser scale, C^{k+1} as given in equation (2.10) and a signal coding the difference in the information, D^{k+1} as given in equation (2.11).

$$C^{k+1}(i) = \sum_n H(n-2i)C^k(n) \quad (2.10)$$

$$D^{k+1}(i) = \sum_n G(n-2i)D^k(n) \quad (2.11)$$

where, H and G are the filter coefficients.

Above operations provide temporal multiscale decomposition. Thresholding is carried out to generate the change detection map. These change detection maps are binary images containing the pixel intensities either 0 or 255 (for 8-bit images). From the simulation, it is found that wavelet based detection algorithm is able to detect high contrast targets but is not suitable for dim point targets.

The intensity differential (gray scale value) between targets and background for simulated image sequences is calculated and data show that if intensity differential is below 80 (on 8-bit image frame), wavelet based algorithm is not able to detect point targets.

2.2.4 IMAGE-DIFFERENCING AND CONTOUR EXTRACTION BASED DETECTION ALGORITHM

This algorithm [22] includes two modules, namely region of interest (ROI) locating and contour extraction. In the former module, image-differencing technique is employed on consecutive images to generate rough candidates of targets appearing in the images. Next, an encoding technique is devised to effectively remove noise that usually severely affects the performance of system. By assuming noise to be Gaussian-distributed, it is concluded that pixels surrounded by three or less than three non-zero neighbors need to be examined in a difference image. From this point of view, the method encodes every pixel and its neighbors and then builds a histogram to determine noise threshold in the difference image.

2.2.5 DETECTION OF DIM SMALL TARGETS BASED ON FRAME CHANGE DETECTION AND TOP-HAT ALGORITHMS

This algorithm for detecting a manoeuvring IR point target in complex background based on frame change detection is proposed in [17]. Small IR targets are disturbed by the background and noise, which results in low SCR and brings difficulty to target detection. In this algorithm, firstly the mathematical morphology filtering based top-hat transform is used to suppress the background of the digital infrared image. Then the union resulted from White Top-Hat Transform (WTT) and Black Top-Hat Transform (BTT) is computed [18]. And then, using adaptive threshold segmentation algorithm, the image is obtained which contains the small targets.

2.2.6 FUSION BASED TARGET DETECTION ALGORITHM

In this algorithm [19], firstly, targets are separately detected by two methods based on gray-scale characteristics and direction discreteness, and then merge the detection result to attain suspicious targets. Secondly, candidate targets have accurate positioning according to the variance growth. Finally, the true targets are obtained according to the principle of moving continuity and trajectory consistency of moving targets in the image sequences. In infrared image sequence, background belongs to the low frequency parts and target as well as noise belongs to the high frequency parts. So we can use wavelet decomposition method to separate them. The high frequency reflects details of image that is nonstationary parts such as line, edge and target and so on. The background of infrared image mainly consists of large area and slow changes region as well as some basic geometric structures such as texture, edge and lines. However, small target has a very small area that only occupies a single pixel or few pixels and there is no structural information such as shape, size and texture, etc.

2.2.7 PARTICLE FILTER BASED SMALL TARGET DETECTION ALGORITHM

Particle filter based detection algorithms have been reported in [23-24]. Firstly, a particle filter based algorithm [23] utilizes a Bayesian based particle filter to track the target in image sequence and get the target search window. Then the detection is performed on the image intensity surface of search window fitted by cubic facet model. The partial derivative operators are exploited according to

cubic facet model to detect maximum intensity points from search window, which correspond to the small target position in image. The searched small target under sky background appears brighter than its neighbour in image sequence, which forms an approximately symmetric convex on the image intensity surface. As the target is very small, the centre of the target position is corresponding to the highest intensity pixels in the small neighbourhood, which locates at the maximal extremum points of the corresponding convex surface. Thus the target can be detected from the background by examining the features of the location. In this way, the small target detection procedure is turned into finding the maximal extremum points on the infrared image intensity surface.

A common problem with the sequential importance sampling particle filter is the degeneracy phenomenon, where after a few iterations, all but one particle will have negligible weights. In addition to choosing better proposal distributions in the sequential importance sampling step, another crucial step in designing the particle filter is selective resampling. The resampling philosophy is to eliminate particles with low importance weights and multiply particles with high importance weights, thus improving the effective particle size.

3 PROPOSED ROBUST LONG RANGE TARGET DETECTION ALGORITHM

Airborne threats like aircrafts and missiles at longer ranges appear as point and small targets in visible and infrared image sequences. Because of the lack of a priori information about target dynamic and structural information such as shape, the detection of such targets becomes extremely challenging. Most of the detection algorithms for example [15-16] are only suitable for a particular kind of background scenario and hence are unable to adapt their behaviour to perform robustly in the rapidly changing environment. In addition, the high computational complexity of reported detection algorithms requires complex processing hardware and leaves little scope for real time implementation. Hence, a novel and robust small target detection algorithm based on Adaptive Selective Double Structuring element Top-Hat Transform (Adapt-Sel-DSTHT) is proposed here. Experimental results show estimation of background close to actual background as well as high probability of detection and low false alarms even for highly clouded scenario. The simplified block diagram and flow diagram of the proposed robust long range target detection algorithm for infra-red and visible image sequences is shown in Figure 3.1 and 3.2 respectively.

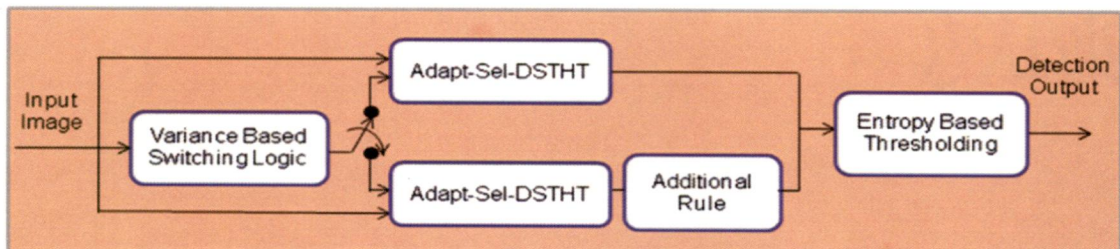


Figure 3.1: Block Diagram of Proposed Robust Long Range Target Detection Algorithm

3.1 PRE-PROCESSING ALGORITHM

Classical mathematical morphological filters are inefficient if the clutter is heavy and the target is dim due to the defect of image detail smoothing. The use of two same structuring elements in classical white top-hat transform cannot differentiate the target and background very well. Because of use of two same structuring elements, all pixels of the structuring element are used for the top-hat transformation calculation and leading to increase in false alarms. To improve the

performance and reduce the number of operations, Adaptive Selective Double Structuring element White Top-Hat Transform (Adapt-Sel-DSTHT) is proposed.

Let f represents a gray-scale image, $B_s(\Delta)$ and $\Delta B(\Delta)$ represent selective SE by considering alternate elements and contour SE of adaptive SE of size Δ . The proposed Adapt-Sel-DSTHT is defined by equation (3.1).

$$\text{Adapt - Sel - DSTHT}_k(x, y) = f_k(x, y) - (f \bullet \Delta B(\Delta)) \circ B_s(\Delta)$$

- gray scale dilation
- where \circ gray scale erosion
 k frame number

$$B_s(\Delta) = \begin{cases} 1, & (x + 2i, y + 2j) \text{ where } i, j \in \left[-\left\lfloor \frac{\Delta-1}{4} \right\rfloor, \left\lfloor \frac{\Delta+1}{4} \right\rfloor \right] \\ 0, & \text{otherwise} \end{cases} \quad (3.1)$$

where Δ size of SE

$\Delta = \text{maximum target size detected in } (k-1)^{\text{th}} \text{ frame} + \varepsilon$

ε : constant

By considering $B_s(\Delta)$ as given in equation (3.1) reduces the number of operations by half as well as predicts the background very close to actual background.

3.2 DETECTION ALGORITHM

Performance of top-hat transform is highly dependent on shape and size of the structuring element (SE) and consequently affects the performance of detection algorithm in terms of probability of detection and false alarm rate. Approaching target results in increase of target size in input image. Keeping the size of SE fixed results in either miss detections or false alarms. By adaptively varying the size of SE for Adapt-Sel-DSTHT based pre-processing improves the overall performance of the detection algorithm.

The output of the Adapt-Sel-DSTHT may be modified by an additional rule to predict the background close to the actual depending on the variance of the input image frame and hence reduces the false alarms for highly cluttered background scenario. The addition rule used for reduction of false alarm is described as follows. The difference between the maximum and minimum gray scale intensity over a window in input image frame acts as deciding value. Then the gray scale

intensity of filtered image is compared with calculated deciding value. If it is greater than the deciding value then the pixel intensity of filtered image is replaced by zero pixel intensity, otherwise gray scale intensity of corresponding filtered image is not modified.

Then maximum correlation criterion [25] of the filtered image is used to generate the optimal threshold value for adaptive thresholding. Hence, we can detect approaching targets robustly in the changing scenario with reduced number of operations. The optimal threshold is established as defined by equation (3.2).

$$\lambda = \left| \max_{i \in G_m} [2.0 * \ln(p(i)(1-p(i))) - \ln(g(i) * g'(i))] \right|, G_m \equiv \{0, 1, 2, \dots, m-1\} \quad (3.2)$$

$$\text{where } p(i) = \sum_{k=0}^i p_k$$

$$g(i) = \sum_{k=0}^i p_k^2$$

$$g'(i) = \sum_{k=i+1}^{m-1} p_k^2$$

$$p_k = \frac{f_k}{M \times N}; f_k : \text{Number of Pixels with Gray Value, } k$$

M : Image Height, N : Image Width

3.3 PERFORMANCE MEASURES

To demonstrate the performance of pre-processing algorithm, a measure named mean absolute value of residual background (MARB) and local signal to clutter ratio (SCR) are used. They are defined by equations (3.3) and (3.4) respectively. Smaller value of MARB states better clutter elimination capability of pre-processing algorithm.

$$\text{MARB} = \frac{\sum_{x \in M, y \in N} |f(x, y) - H_f(x, y)|}{M \times N}$$

$$\text{where } \begin{array}{l} f \text{ Input Image} \\ H_f \text{ Filtered Image} \\ M \text{ Image Height} \\ N \text{ Image Width} \end{array} \quad (3.3)$$

$$SCR = \left\{ \frac{1}{\sigma_B^2} \sum_{i \in W} \sum_{j \in W} [f(x-i, y-j) - \mu_B] \right\}$$

where σ_B^2 and μ_B are Variance and Mean of the Background (3.4)
 (x, y) is the Pixel of Interest

To evaluate the performance of detection algorithm two measures named probability of detection (P_d) and probability of false alarm (P_f) are used as given by equations (3.5) and (3.6) respectively.

$$P_d = \frac{N_c}{N_t}, \quad (3.5)$$

$$P_f = \frac{N_f}{N_t + N_f} \quad (3.6)$$

N_c : Number of Correct Detection

N_f : Number of False Alarm

N_t : Total Number of True Targets

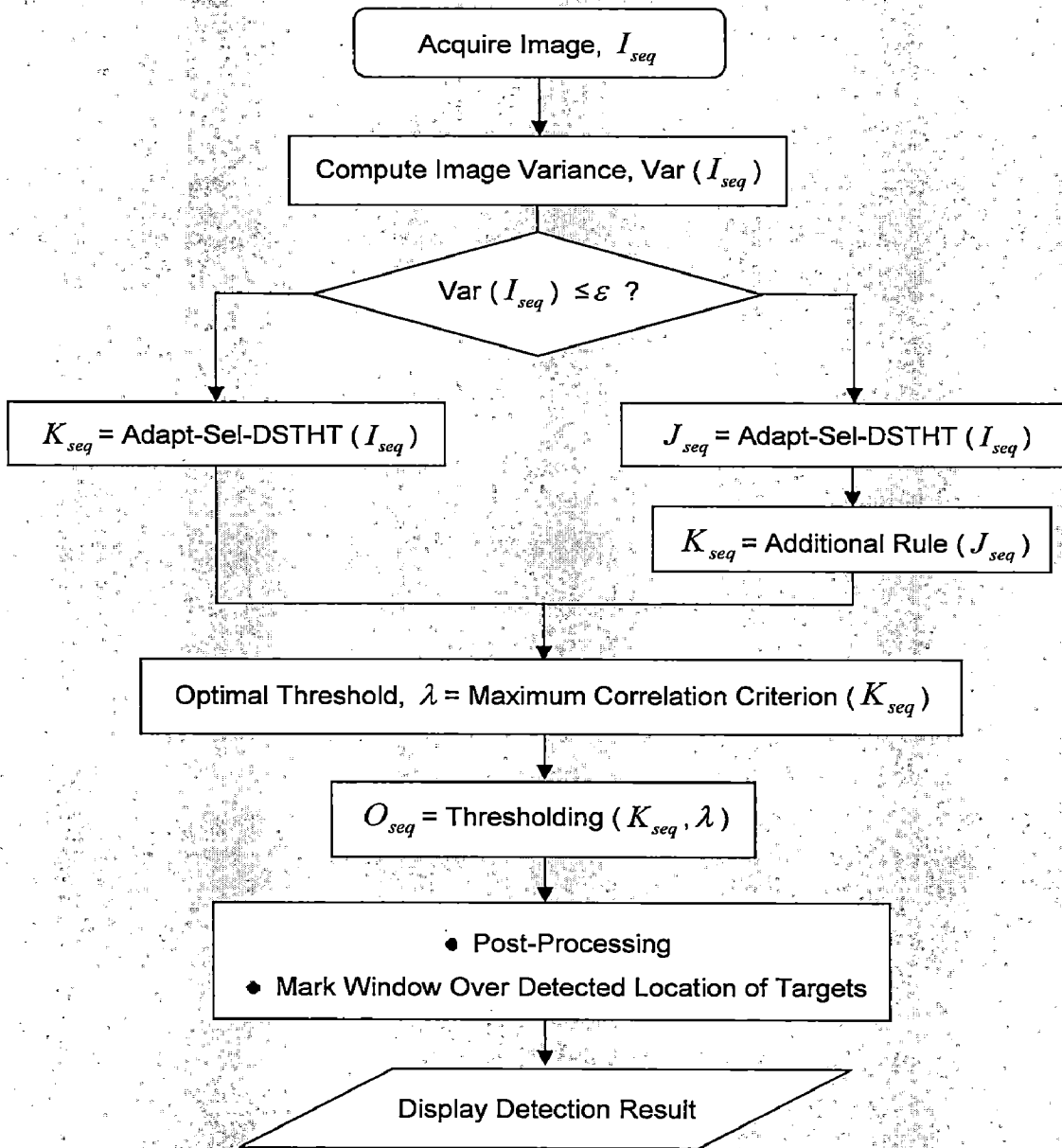


Figure 3.2: Flow Diagram of Proposed Robust Long Range Target Detection Algorithm

4 SIMULATION METHODOLOGY AND RESULTS

The pre-processing and detection algorithm for detection of point and small targets were implemented using MATLAB programming [26]. MATLAB is a high-performance language for technical computing. It integrates computation, visualization, and programming in an environment where problems and solutions are expressed in familiar mathematical notation to solve the technical computing problems. A graphical user interface (GUI) for the proposed long-range airborne target detection system is developed using MATLAB event-driven programming [27]. The important implementation tasks are listed below.

- Implementation of pre-processing and detection algorithms for detection of point or small airborne targets
- Programming to develop Graphical User Interface (GUI) for interactive human-machine interface
- Programming to interface the video sensor (camera) for real-time (online) capture and processing of image frames

4.1 GRAPHICAL USER INTERFACE DESIGN

Graphical user interface (GUI) for the pre-processing and detection algorithm developed/implemented is ALoRT-DetSys (Advanced Long Range Target Detection System). ALoRT-DetSys has been designed and developed using MATLAB programming and MATLAB event-driven programming. Snapshots of the ALoRT-DetSys are shown as Figure 4.1 and 4.2. In event-driven programming, callback execution is asynchronous, controlled by events external to the software. The input parameters required for pre-processing and detection algorithms are provided interactively through GUI. The GUI design for ALoRT-DetSys is based on followings.

- Identification of important input and output parameters, required to test and run the Pre-Processing Algorithms and AMCE Based Detection Algorithm
- Enable (or Disable) the relevant (irrelevant) options.
- Grouping of common functions under same frame.

- Programming and interface of video camera to online capture and processing of image frames to detect point and small IR targets.

The salient features of the ALoRT-DetSys GUI are listed below.

- GUI for pre-processing algorithms and detection algorithms
- Facility to process the image frames offline (stored frames)
- Facility to online Target capture of image frames by video camera and their processing to detect point and small targets
- Facility to take the snapshots from the connected video camera and to save in standard image file formats.
- Online selection of options to show various results while processing is in progress. For example, user can select “Show Pre-Processing Result” to see the result of pre-processing algorithm.
- Online selection of options to save various results. For example, user can select “Save Difference Image” to save the difference image.
- Marking of window around detected position of targets and display of their position (spatial coordinates) and size of the targets.
- Storing of candidate target list for offline analysis thereafter.
- Help for simulated pre-processing algorithms and detection algorithm.

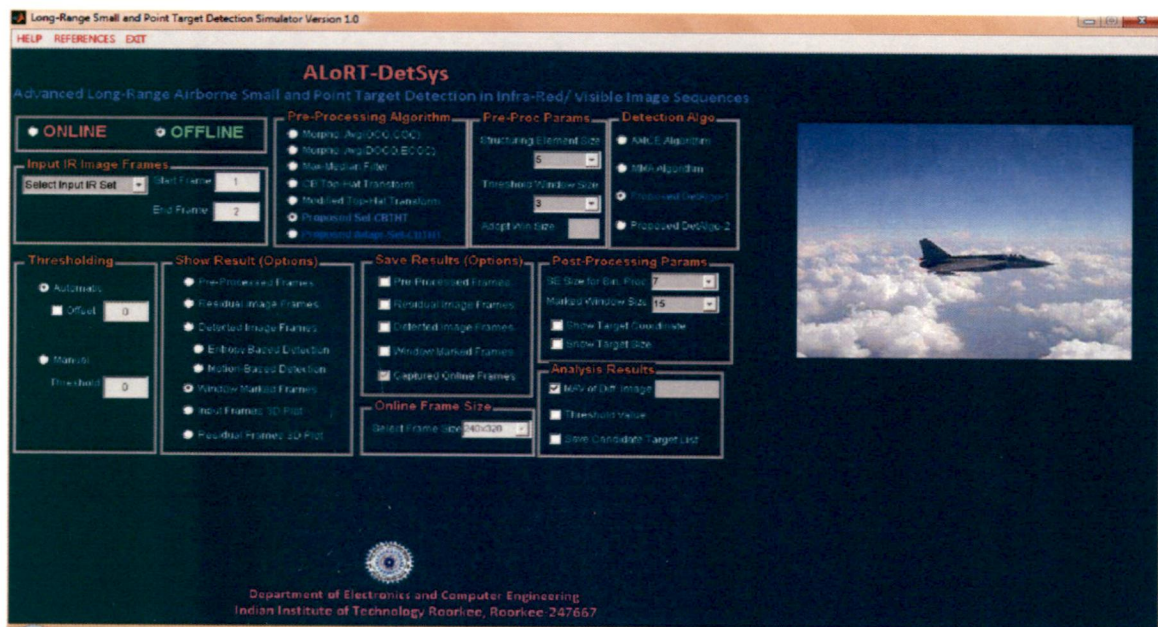


Figure 4.1: Snapshot of the GUI of the ALoRT-DetSys

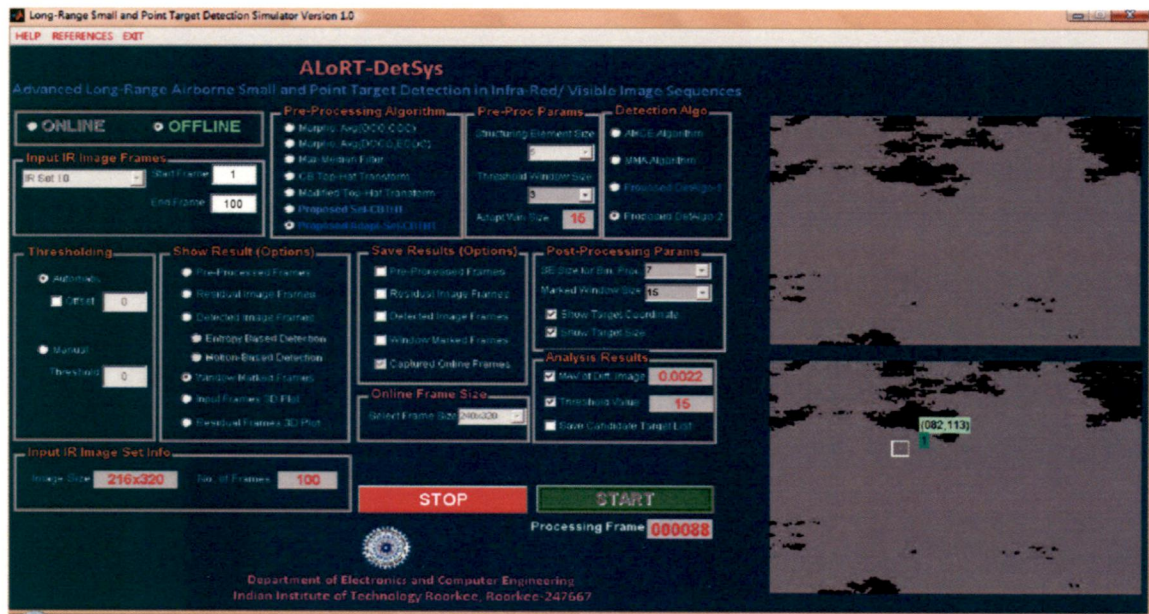


Figure 4.2: Snapshot of the GUI of the ALoRT-DetSys during Processing

4.2 SIMULATION SETUP

The proposed ALoRT-DetSys has the capability to process stored image sequences as well as online capture of image frames by a camera (video sensor) and then applying the detection algorithms to detect point and small targets. The experimental setup for processing of online image frames is given in Figure 4.3. Snapshot of the ALoRT-DetSys GUI during online processing is shown in Figure 4.4.



Figure 4.3: Simulation Setup of ALoRT-DetSys for Online Processing

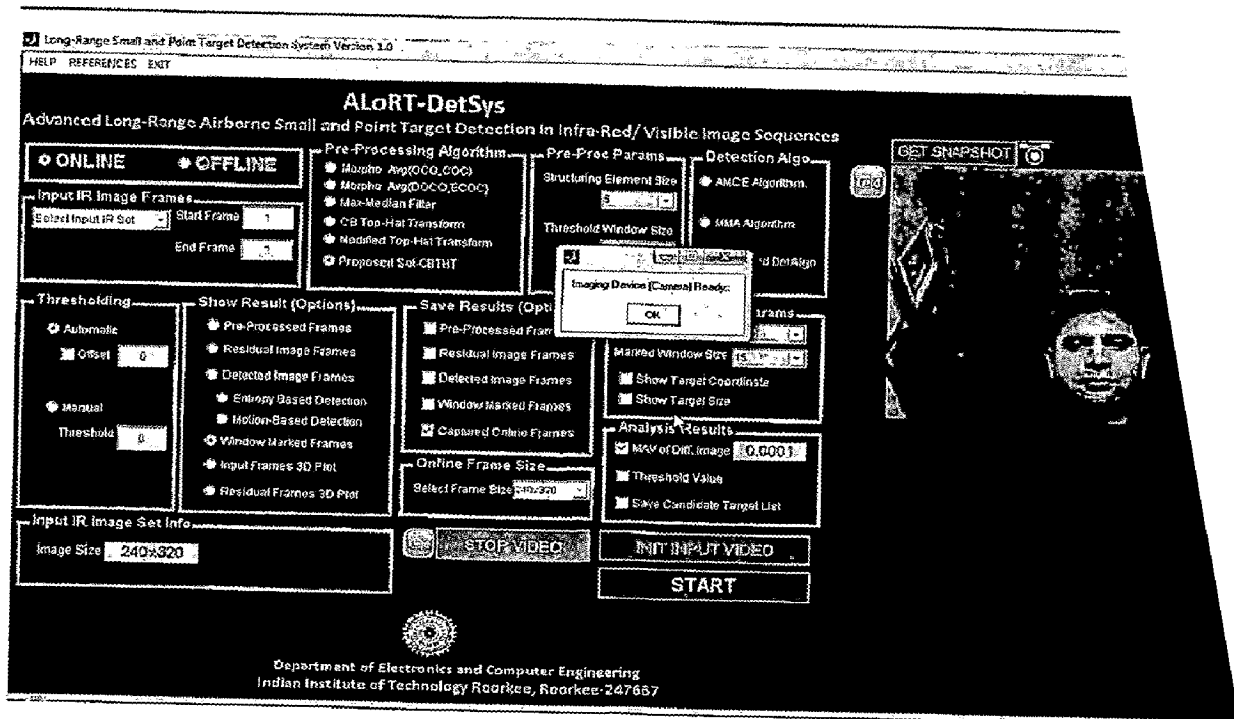


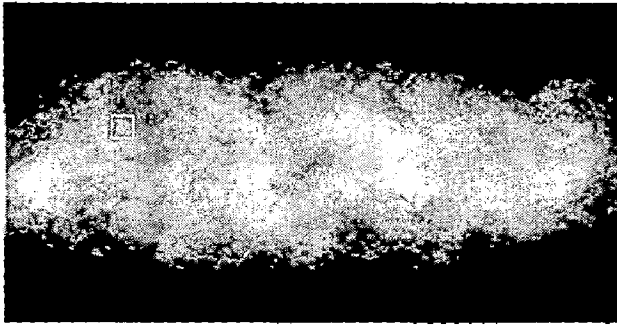
Figure 4.4: Snapshot of the GUI of the ALoRT-DetSys for Online Processing (Testing/Initialization)

4.3 RESULTS AND PERFORMANCE COMPARISONS

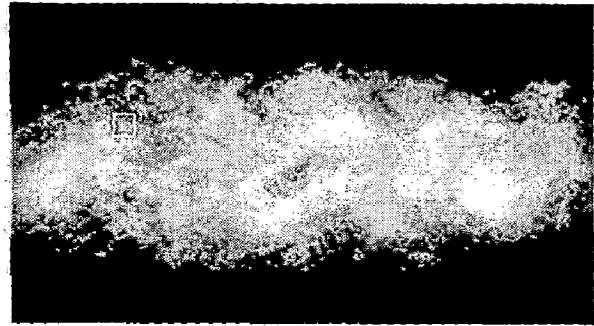
To verify the efficiency of the pre-processing and detection algorithms, these are tested for many real and synthetic image sequences. Synthetic points as well as extended size targets (upto 5x5 pixels) have been embedded into synthetic as well as real image sequences to measure the performance. Separate performance evaluation of pre-processing filters as well as with detection algorithms has been performed.

1 SIMULATION RESULTS OF PRE-PROCESING ALGORITHMS

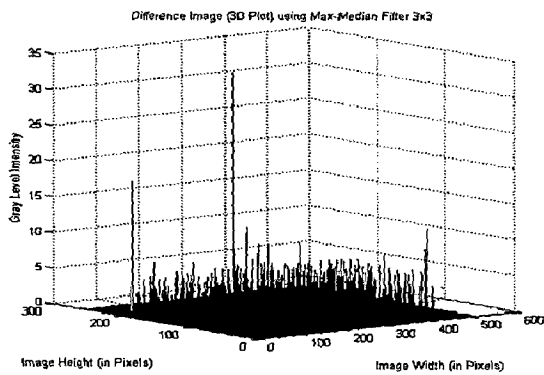
The performance of the pre-processing algorithms can be evaluated based on the two parameters called Mean Absolute value of Residual Background (MARB) and Signal to Clutter Ratio (SCR) as discussed in Section 5.3. The simulation results for sample image frames by Max-Median Filter, Morphological Filter (open), CB Top-Hat Transform and the proposed Adapt-Sel-DSTHT filter (for two different image frames) are presented in Figure 4.5 to 4.9 respectively.



(a)



(b)

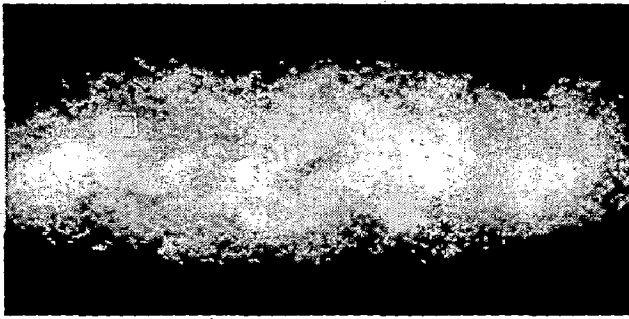


(c)

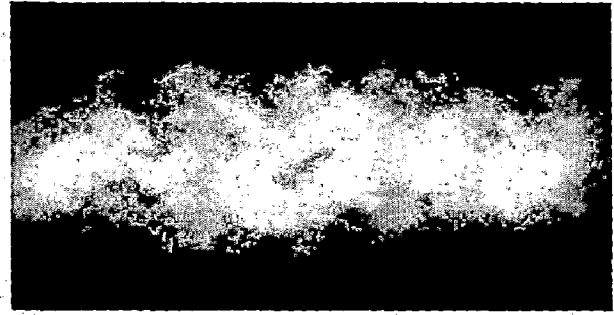
Simulation Statistics:
Input SCR : 1.3043
Output SCR : 34.00
MARB : 0.0149

(d)

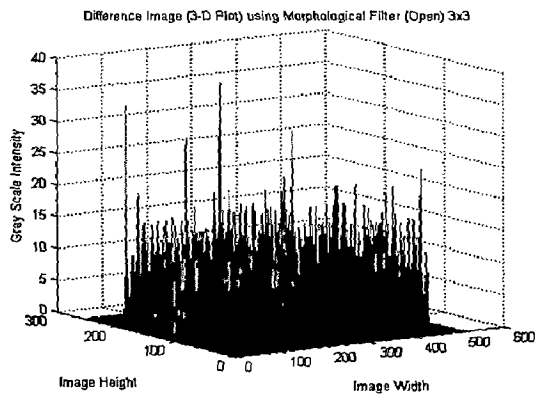
Figure 4.5: Pre-Processing Result (a) Input Image Frame, (b) Max-Median Filtered Frame, (c) 3D Plot of Difference Image, (d) Simulation Statistics



(a)



(b)



(c)

Simulation Statistics:

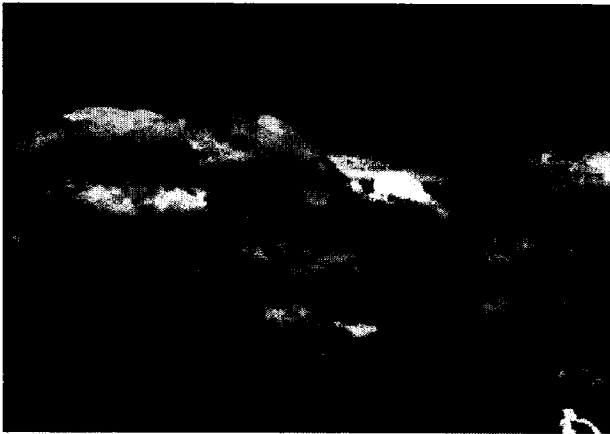
Input SCR : 1.3043

Output SCR : 28.5014

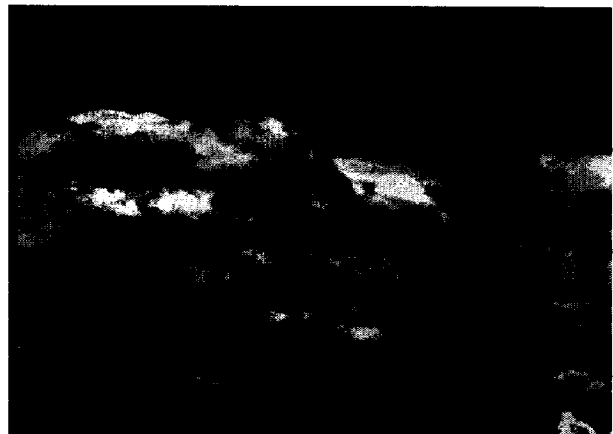
MARB : 1.0911

(d)

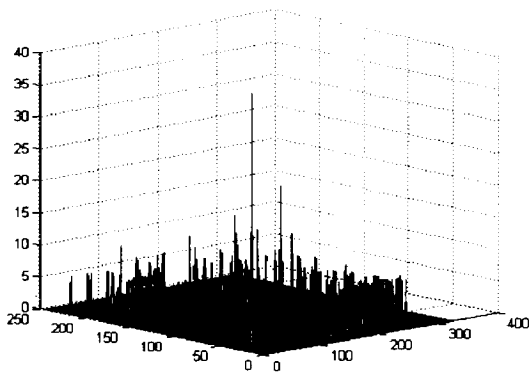
Figure 4.6: Pre-Processing Result (a) Input Image Frame, (b) Morphological Opened Frame, (c) 3D Plot of Difference Image, (d) Simulation Statistics



(a)



(b)



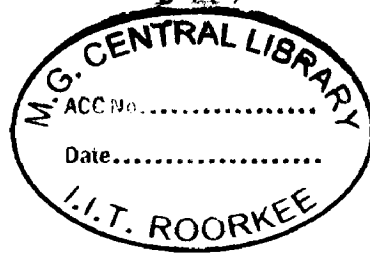
Simulation Statistics:

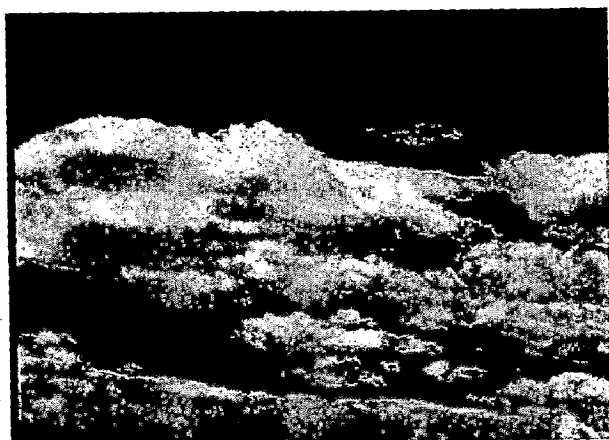
Input SCR : 0.9390

Output SCR : 32.00

MARB : 0.0403

Figure 4.7: Pre-Processing Result (a) Input Image Frame, (b) CB White Top-Hat Transform Frame, (c) 3D Plot of CB Top-Hat Transform Image, (d) Simulation Statistics

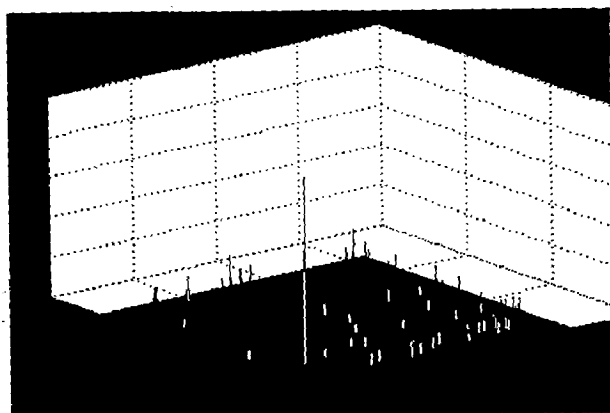




(a)

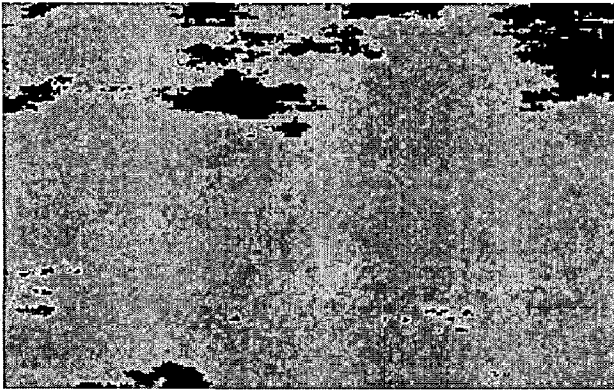


(b)

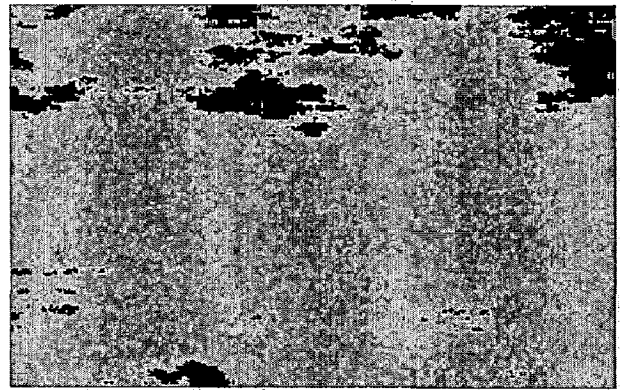


Simulation Statistics:
Input SCR : 0.9390
Output SCR : Inf
MARB : 0.0301

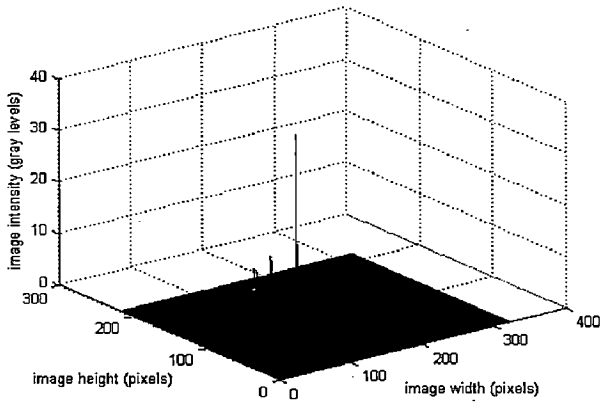
Figure 4.8: Pre-Processing Result (a) Input Image Frame, (b) Proposed Selective-Double Structuring Element Top-Hat Transform (Adapt-Sel-DSTHT) Frame, (c) 3D Plot of Adapt-Sel-DSTHT Image, (d) Simulation Statistics



(a)



(b)



Simulation Statistics:
Input SCR : 5.105
Output SCR : Inf
MARB : 0.0104

Figure 4.9: Pre-Processing Result (a) Input Image Frame, (b) Proposed Selective-Double Structuring Element Top-Hat Transform (Adapt-Sel-DSTHT) Frame, (c) 3D Plot of Adapt-Sel-DSTHT Image, (d) Simulation Statistics

Test results for five image sequences of different scenario are used for performance evaluation. Each image sequence has 100 image frames. Two synthetic targets of size 3x3 pixels are embedded in each image frame of image sequences 1, 2, 3 and 5. Image sequence 4 has one point (pixel) target in each image frame. Performance of the proposed Adapt-Sel-DSTHT filter is evaluated against MARB and compared with max-median filter, morphological filter (Open) more specifically white top-hat transform, and new top-hat transform (NTHT). The values of MARB are plotted and shown in Figure 4.10. Plot for proposed Adapt-Sel-DSTHT filter demonstrates lowest MARB and hence estimation of background very close to actual background and hence leads to superior performance of detection algorithm even for highly cluded background.

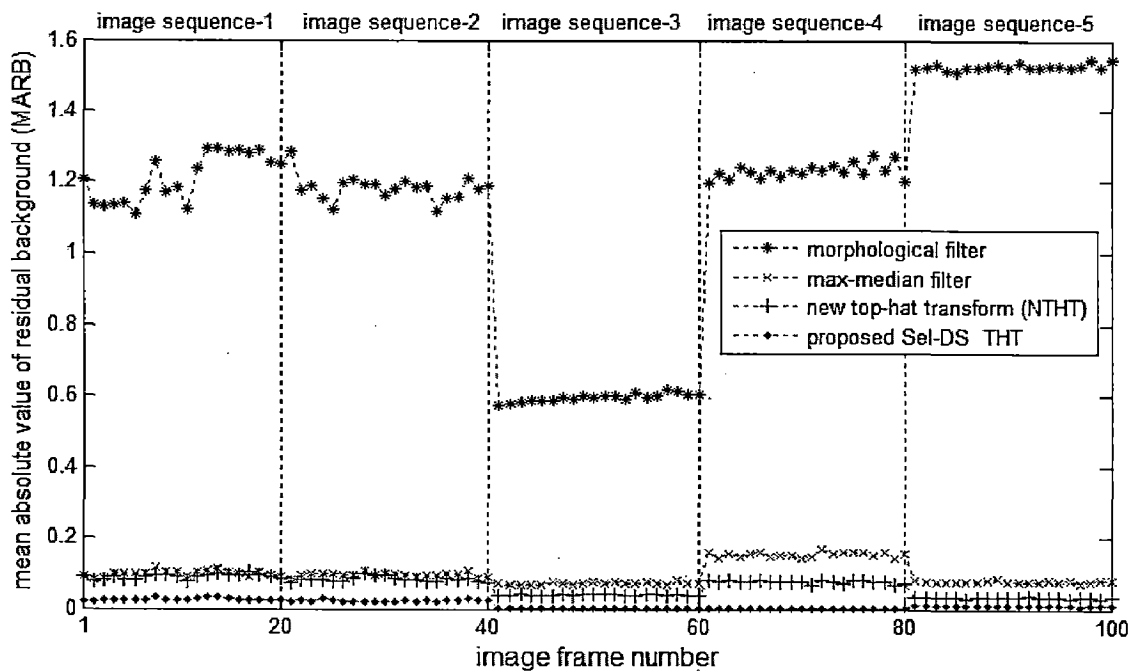
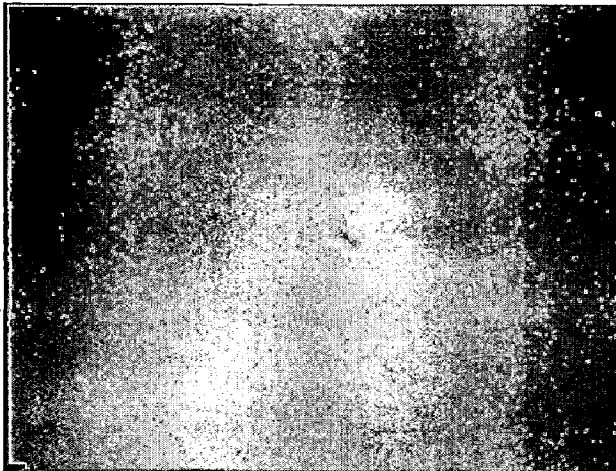


Figure 4.10: Plot of MARB for Image Frames for Max-Median Filter, Classical Morphological Filter, New Top-Hat Transform, and the Proposed Adapt-Sel-DSTHT

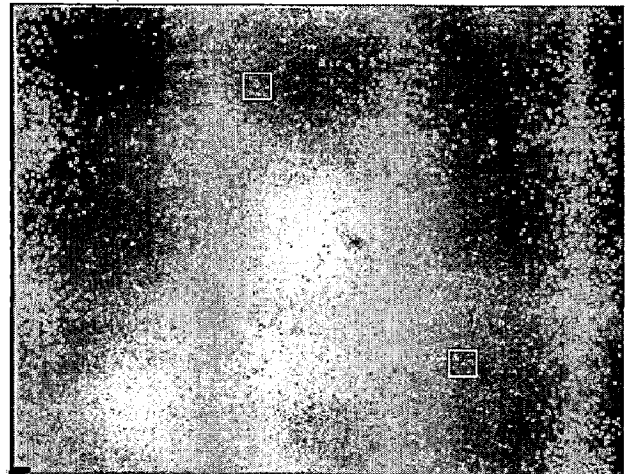
4.3.2 SIMULATION RESULTS OF DETECTION ALGORITHMS

Two measures named probability of detection and probability of false alarm are used to evaluate the overall performance of the proposed detection algorithm. Test results for five image sequences of different scenario are used for performance evaluation. Each image sequence has 100 image frames. Each

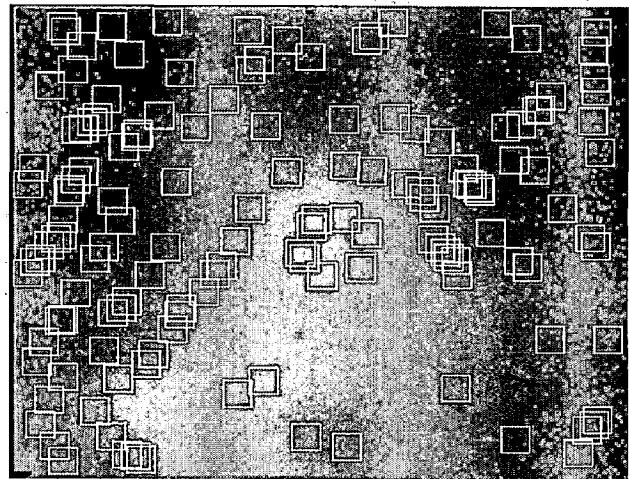
frame of Image Sequences 1 to 5 has two point targets. Image sequences 1 and 2 have high spatially correlated background with less variance value (typically ≤ 35) while others have dense cloudy background with high variance value. Detection results of sample frame of each Image Sequence (namely Image Sequence 1, 2, 3, 4 and 5) are shown in Figure 4.11 to 4.15 respectively. To test the performance of proposed detection algorithm for extended size targets, synthetic targets of size 3x3 pixels as well as 5x5 pixels are embedded in Image Sequence 1 and the detection results are shown in Figure 4.16 and 4.17 respectively.



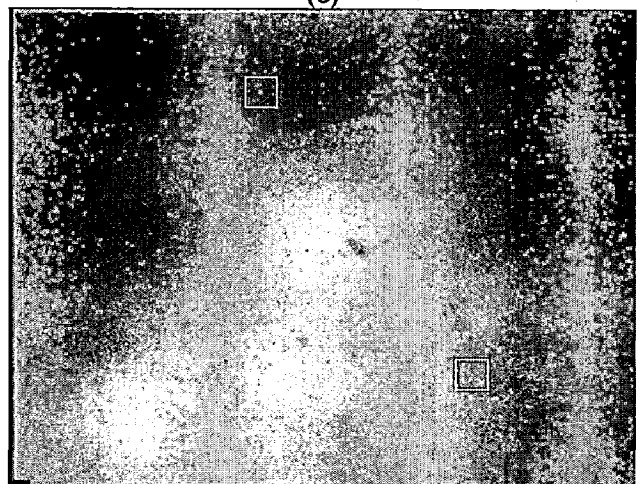
(a)



(b)



(c)

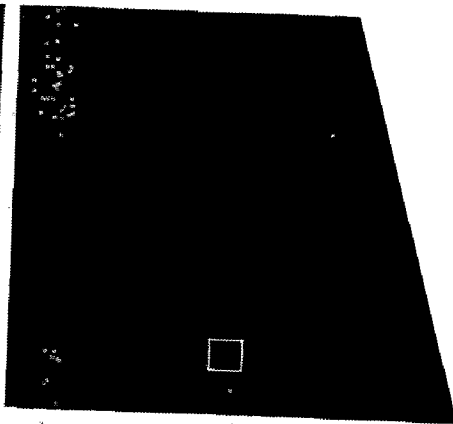


(d)

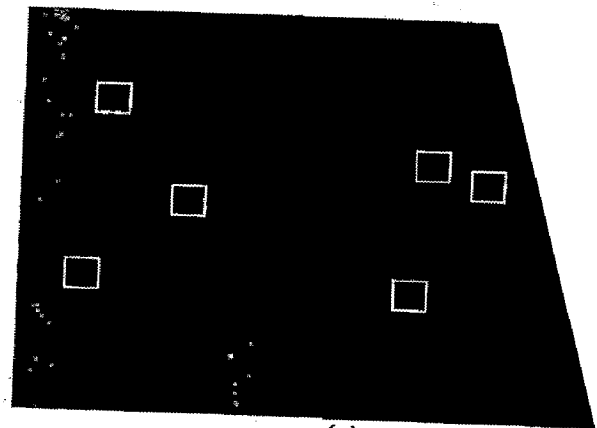
Figure 4.11: Detection Results of Image Sequence 1: (a) Input Frame, (b) Detection Result of MMA Algorithm, (c) Detection Result of AMCE Algorithm, (d) Detection Result of Proposed Robust Target Detection Algorithm



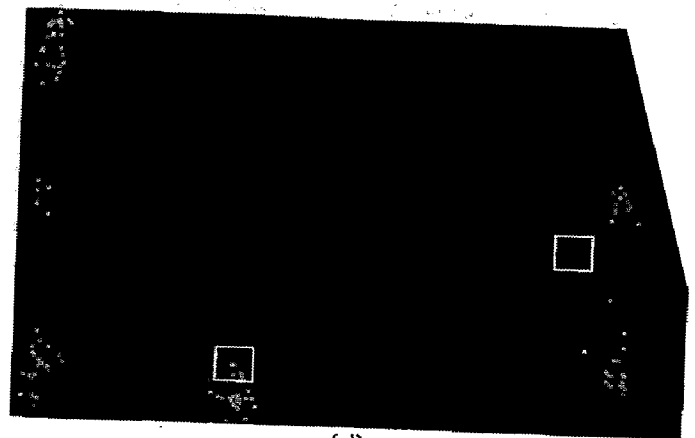
(a)



(b)

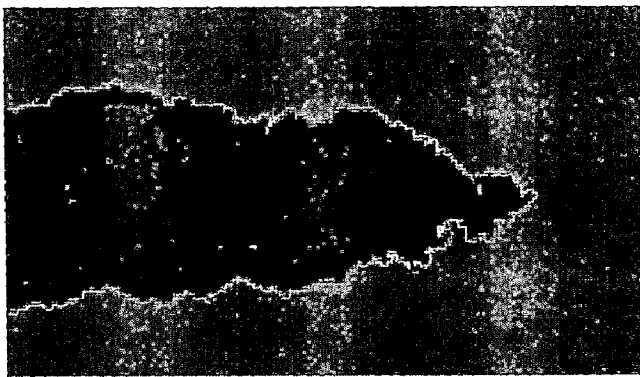


(c)

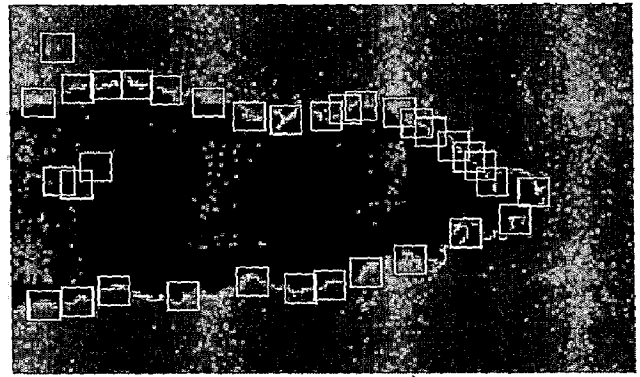


(d)

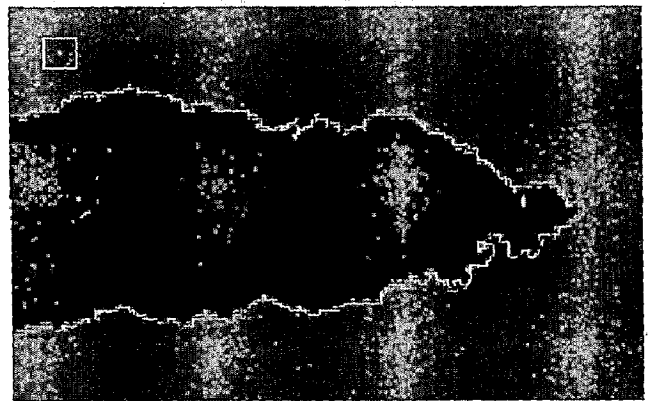
Figure 10. Detection Results of Image Sequence 2 (a) Input Frame, (b) Detection Result of MMA, (c) Detection Result of AMCE Algorithm, (d) Detection Result of Proposed Robust Target Detection Algorithm



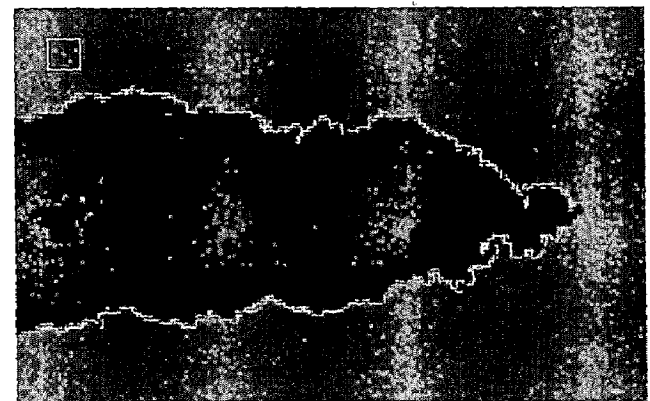
(a)



(b)

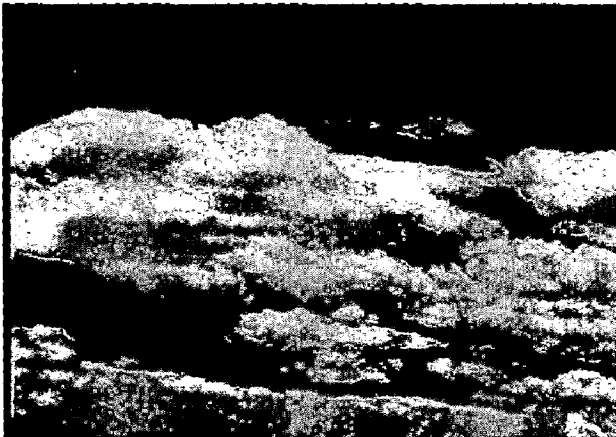


(c)

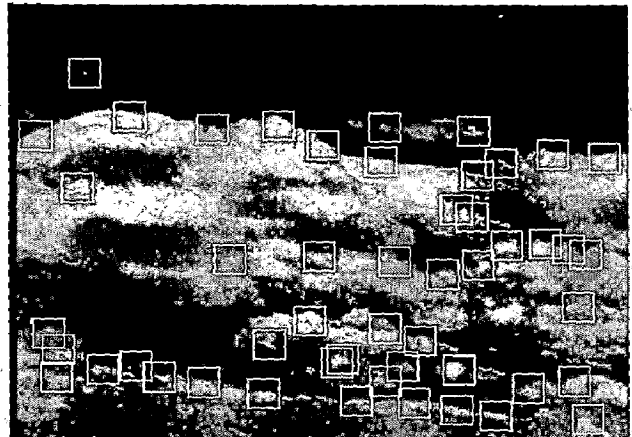


(d)

Figure 4.13: Detection Results of Image Sequence 3 (a) Input Frame, (b) Detection Result of MMA Algorithm, (c) Detection Result of AMCE Algorithm, (d) Detection Result of Proposed Robust Target Detection Algorithm



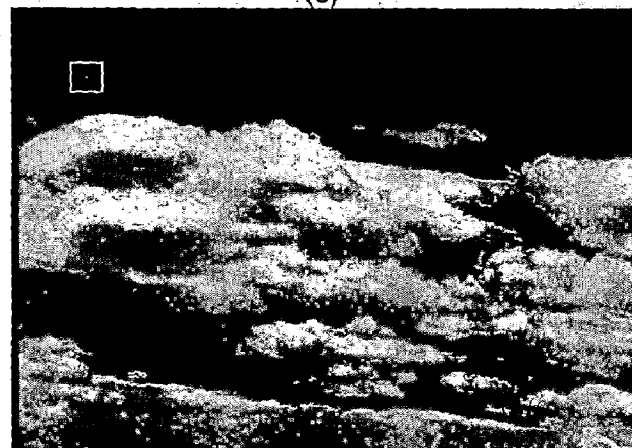
(a)



(b)

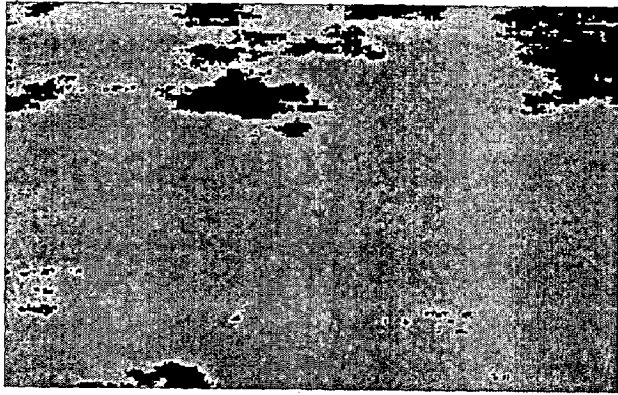


(c)

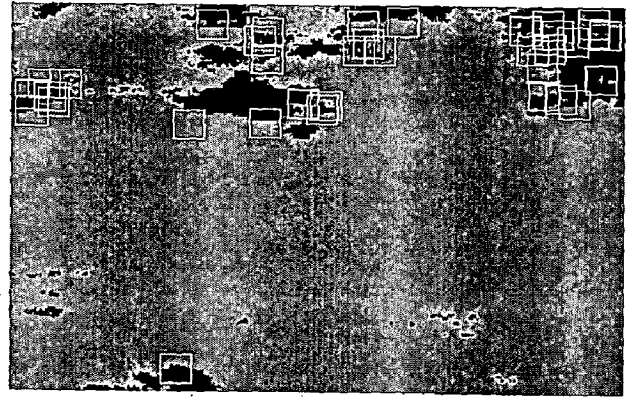


(d)

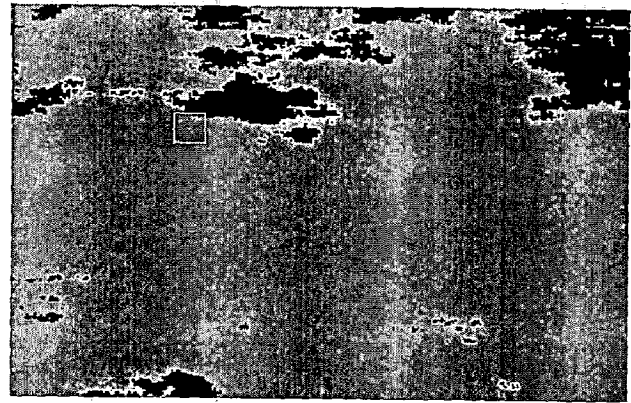
Figure 4.14: Detection Results of Image Sequence 4 (a) Input Frame, (b) Detection Result of MMA Algorithm; (c) Detection Result of AMCE Algorithm, (d) Detection Result of Proposed Robust Target Detection Algorithm



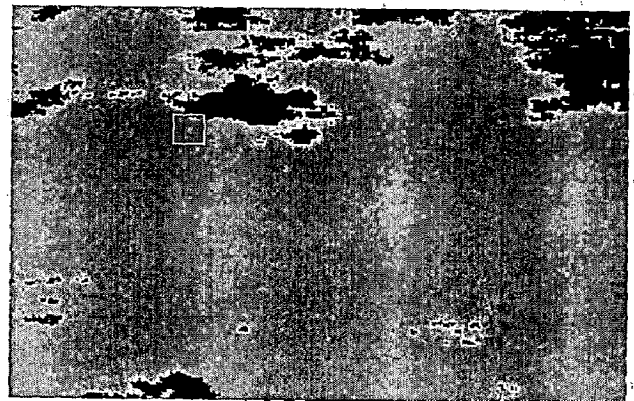
(a)



(b)

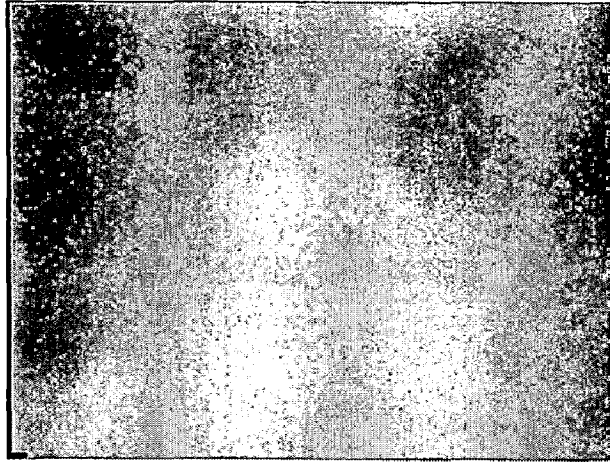


(c)

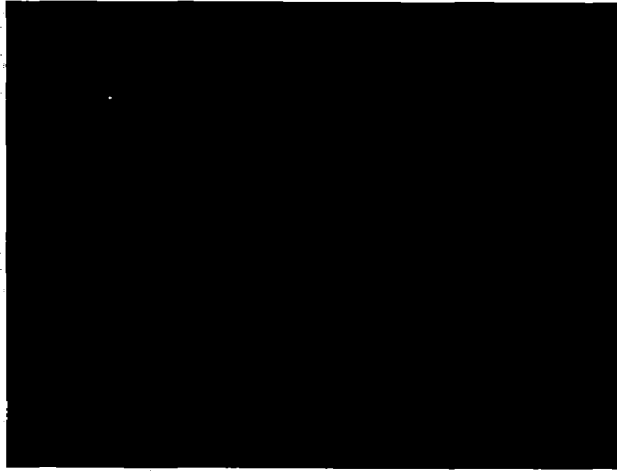


(d)

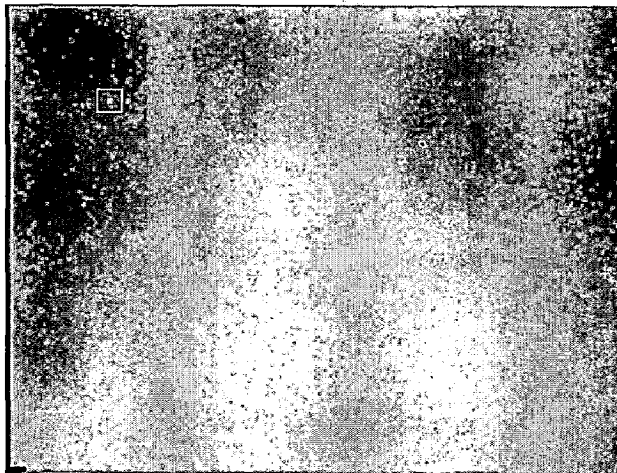
Figure 4.15: Detection Results of Image Sequence 5 (a) Input Frame, (b) Detection Result of MMA Algorithm, (c) Detection Result of AMCE Algorithm, (d) Detection Result of Proposed Robust Target Detection Algorithm



(a)

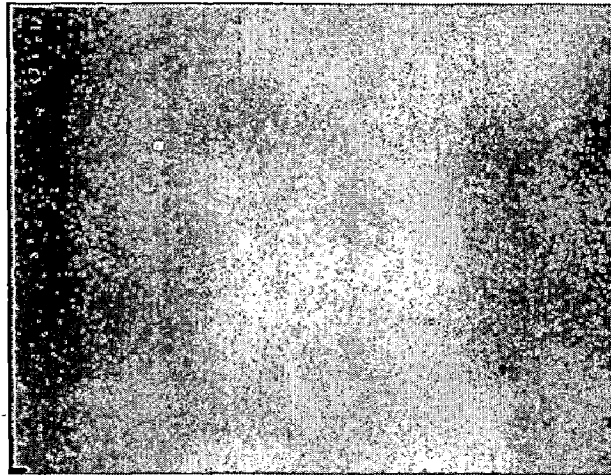


(b)

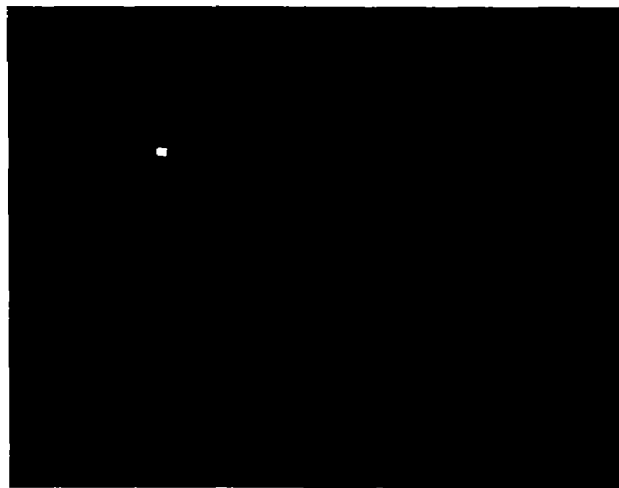


(c)

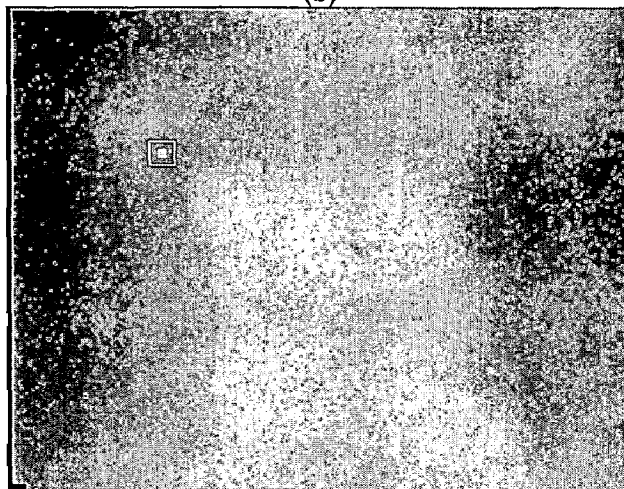
Figure 4.16: Detection Result of Extended Size Target of Size 3x3 Pixels in Image Sequence 1
(a) Input Frame, (b) Binarized Output of Proposed Robust Target Detection Algorithm,
(c) Window Marked Around Detected Position of Target in Input Image



(a)



(b)



(c)

Figure 4.17: Detection Result of Extended Size Target of Size 5x5 Pixels in Image Sequence 1
(a) Input Frame, (b) Binarized Output of Proposed Robust Target Detection Algorithm,
(c) Window Marked Around Detected Position of Target in Input Image

Experimental results of the proposed algorithm are compared with MMA algorithm and AMCE algorithm and given in Table 4.1. Results demonstrate the robust performance of the proposed algorithm under changing background with remarkable high probability of detection ≥ 0.98 and low probability of false alarm < 0.04 . Results conclude very good and robust performance for test image sequences of different scenario.

TABLE 4.1: PROBABILITY OF DETECTION AND PROBABILITY OF FALSE ALARM

| Image Sequence | MMA Algorithm | | AMCE Algorithm | | Proposed Adapt-Self-DSTHT Based Robust Target Detection Algorithm | |
|------------------|---------------|-------|----------------|-------|---|-------|
| | P_d | P_f | P_d | P_f | P_d | P_f |
| Image Sequence-1 | 0.970 | 0 | 0.400 | 0.991 | 1 | 0 |
| Image Sequence-2 | 1 | 0.038 | 0.160 | 0.995 | 0.980 | 0 |
| Image Sequence-3 | 0.920 | 0.899 | 0.940 | 0.129 | 0.980 | 0.039 |
| Image Sequence-4 | 0.300 | 0.994 | 0.960 | 0.076 | 1 | 0 |
| Image Sequence-5 | 0.960 | 0.893 | 0.965 | 0.140 | 0.980 | 0.020 |

5 REAL-TIME IMPLEMENTATION ON POWERPC HARDWARE

Real-Time implementation of proposed Adapt-Sel-DSTHT based robust long range detection algorithm has been successfully done on PowerPC hardware. PowerPC G4 [28] is a 32-bit Reduced Instruction Set Computer (RISC) processor from Motorola Inc. PowerPC G4 family of processor has an additional AltiVec [29] vector processing unit to provide SIMD (Single Instruction Multiple Data) architecture. AltiVec unit of PowerPC G4 significantly speeded up the execution and lead to real-time implementation of proposed robust long range target detection algorithm.

5.1 HARDWARES AND SOFTWARES USED FOR HARDWARE IMPLEMENTATION

- Hardware

- ▶ VME 64x Chassis (Figure 5.1): To House the SVME-183 PowerPC 7447 Board
- ▶ SVME-183 Board [30-31] (Figure 5.2): PowerPC 7447 Processor Card
- ▶ PMC 704 [32] (Figure 5.3): Graphics Input/Output PMC Card for Real-Time Video Acquisition and Display
- ▶ Infra-Red/CCD Video Camera (Figure 5.4): For Video Acquisition

- Software/Programming

- ▶ VxWorks RTOS: Real-Time Operating System with BSP
- ▶ Wind River IDE/GNU C: IDE to Compose and Cross Compile Code
- ▶ X11: Graphics Programming Language

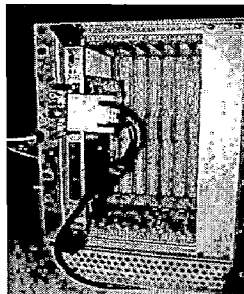


Figure 5.1: VME Chassis

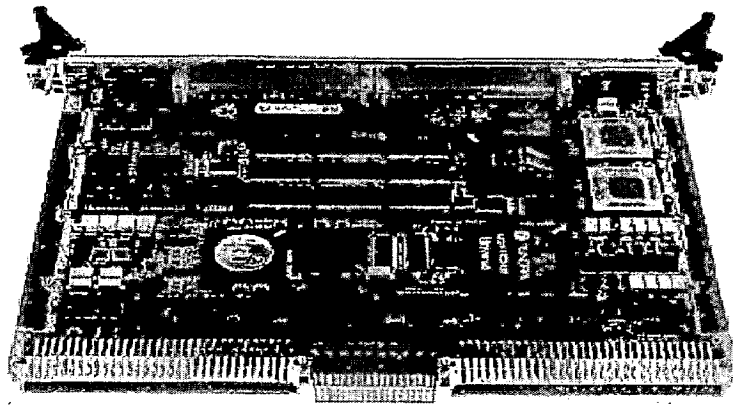


Figure 5.2: SVME 183 PowerPC Board

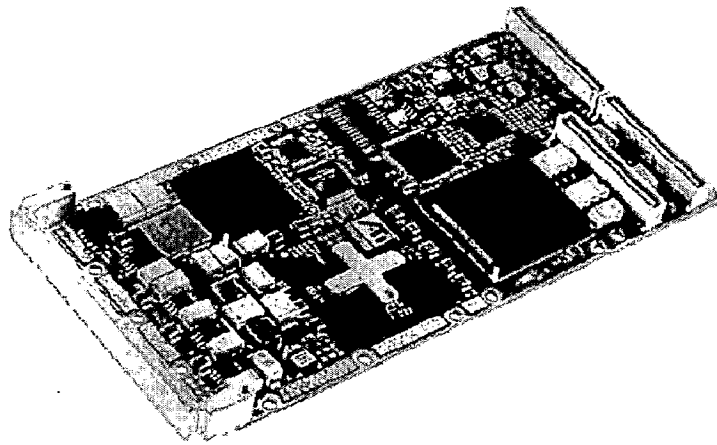


Figure 5.3: PMC 704 Graphics Input/Output Card

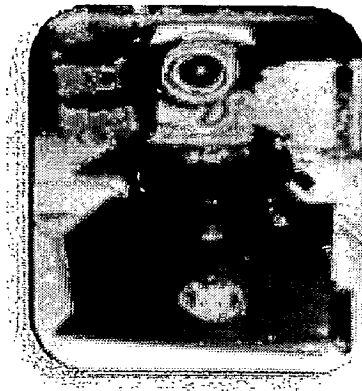


Figure 5.4: Camera Mounted on Scanning Gimbal

Features SVME-183 PowerPC Board

- MPC7447A PowerPC Processor (AltiVec™ Technology)
 - 64 KB L1 cache
 - 512KB/1MB Internal L2 cache
 - AltiVec Vector Processing Unit
 - 9.6 GFLOPS peak processing power at 1.2GHz
- High-performance Discovery III System Controller
 - Dedicated CPU-to-SDRAM Path Reduces Memory Read Latency
- 512MB of DDR SDRAM
- 512MB of Direct-Mapped Flash
 - Hardware Flash Write Protection Jumper
- 128KB AutoStore nvSRAM with Hardware Write Protection
- Three Ethernet interfaces
- Two 64-bit PMCs on Independent PCI Buses
 - One 100MHz PCI-X, one 66MHz PCI-X
- Two Asynchronous RS-232 Serial Ports
- RS-232/422/485 Serial Channels
- Four General-Purpose 32-bit User Timers
- Four General-Purpose PCI/SDRAM DMA Controllers
- Real-Time Clock
- Four On-Board Temperature Sensors
- VME DMA
- VxWorks RTOS and Workbench 2.0

The SVME-183 Core Processing Architecture [31] is given in Figure 5.5.

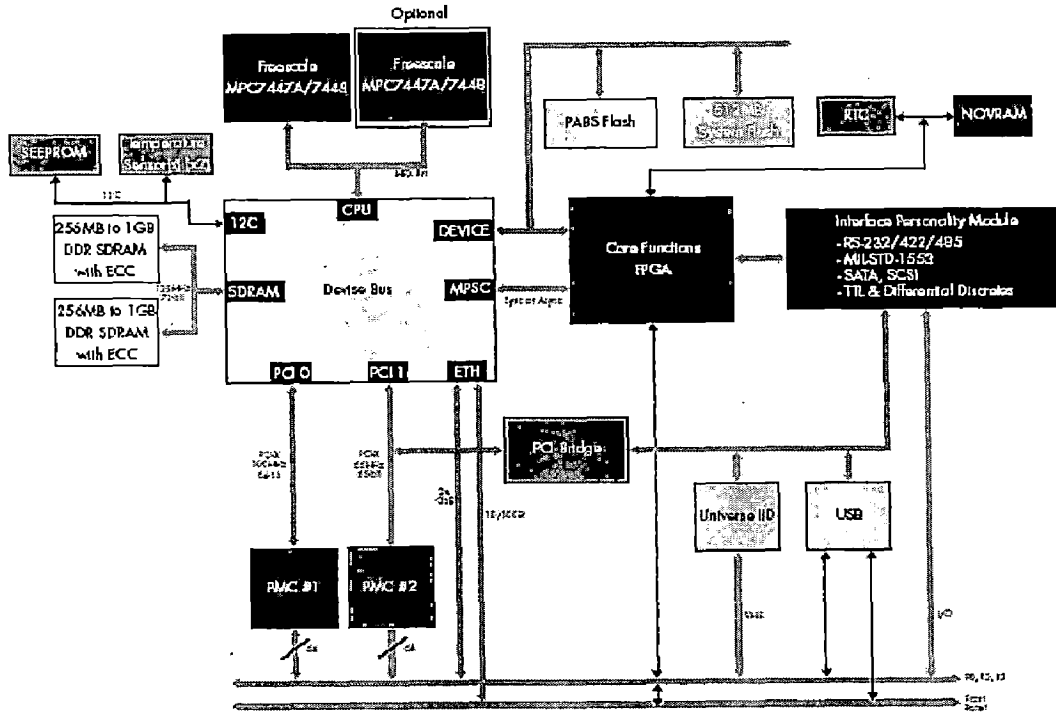


Figure 5.5: SVME-183 Core Processing Architecture

5.2 OVERVIEW OF POWERPC (ALTIVEC)

The PowerPC G4 processor is based on a 32-bit memory model, compatible with the older PowerPC series of processors. The processor has support for two levels of cache. The PowerPC has true superscalar functionality. It can fetch and dispatch more than one instruction per cycle. More than one instruction can be executing in any given cycle. Most instructions execute in a single clock cycle; only a small number of instructions do not have one instruction per cycle throughput. The execution units of PowerPC including Altivec vector unit is shown in Figure 5.6.

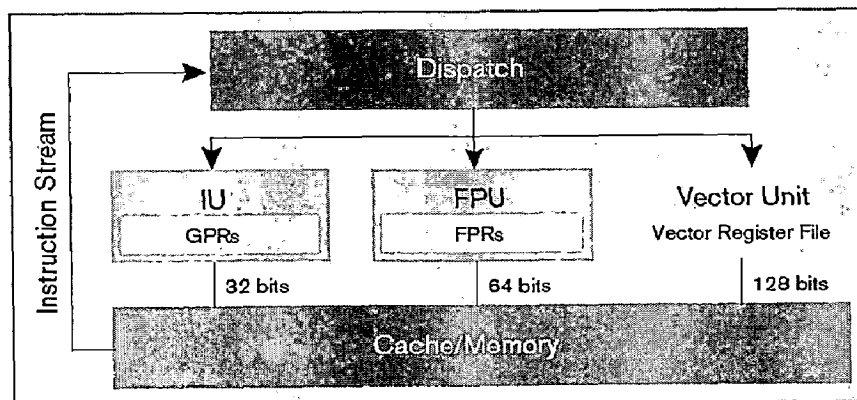


Figure 5.6: Execution Units of PowerPC G4

The AltiVec Technology is one of the most comprehensive implementations of the Single Instruction Multiple Data (SIMD) technology. AltiVec extends the scalar PowerPC architecture with a powerful new set of vector instructions. These instructions execute from the same instruction stream as the PowerPC's scalar integer, floating-point, and branch instructions. AltiVec supports vector-element data types of 8-, 16-, and 32-bit signed or unsigned integers as well as IEEE single-precision floats. Each value within an AltiVec register is a vector that is made up of elements. AltiVec instructions perform simultaneous operations on all elements within an AltiVec vector register. Scalar versus vector processing is shown in Figure 5.7.

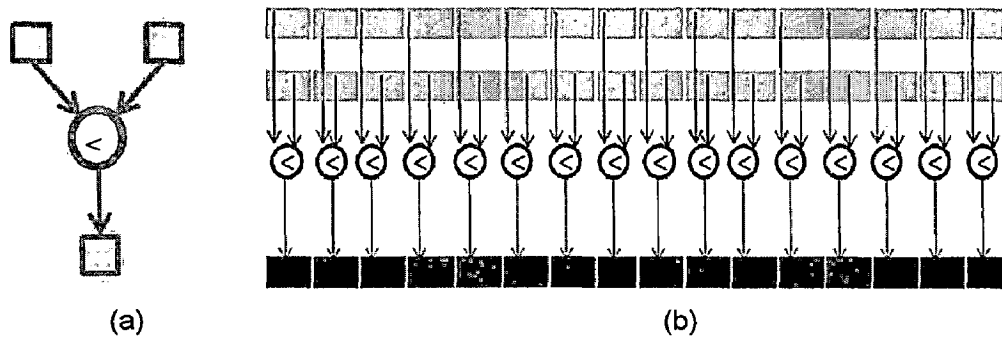


Figure 5.7: (a) Scalar Processing, (b) Vector Processing

5.3 REAL-TIME IMPLEMENTATION OF MORPHOLOGICAL PRE-PROCESSING ALGORITHM USING ALTIVEC

Morphological filters are used as pre-processing algorithm but its use has long been hampered by its algorithmic complexity as the size of the structuring element or image grows. From the simulation, it is found that morphological pre-processing is the bottleneck for real time processing. The performance of morphological processing algorithm can be speedup using AltiVec vector processing unit. The target size in the image sequence increases as the target comes closer to the sensor head. The shape and size of the structuring element affect the detection performance. The scalar constant-time van Herk-Gill-Werman (vHGW) algorithm is based on dividing the image data to overlapping segments of size $2s-1$, centered at $p_{s-1}, p_{2s-1}, p_{3s-1}, \dots$ where, s is the size of 1-D structuring element. The vHGW algorithm performs a dilation or erosion by a 1-D

SE of size $p = 2s-1$. It performs less than three comparisons per pixel regardless of size of structuring element. Let, i be the index of an element at the centre of a certain segment. The maxima of the s elements which include p_i are computed in one batch as follows.

Step 1: Pre-Processing Step

Let
$$R_j = R_j(i) = \text{Max}(p_i, p_{i-1}, \dots, p_{i-j}), \quad j = 0, 1, \dots, s-1 \quad (5.1)$$

$$S_j = S_j(i) = \text{Max}(p_i, p_{i+1}, \dots, p_{i+j}), \quad j = 0, 1, \dots, s-1 \quad (5.2)$$

Step 2: Merging Step

In this step R_j and S_j are merged together to compute the max filter as given by (5.3).

$$T_j = \text{Max}(R_j, S_{s-j-1}), \quad j = 1, 2, \dots, s-2 \quad (5.3)$$

Maximum three comparisons per element are required for 1-D dilation or erosion.

5.3.1 VECTORIZATION METHODOLOGY

In this algorithm, an input image is divided into blocks of overlapping rows. The size of each block is $(2s-1) \times 16$ pixels where s is the size of structure element (SE). The contiguous 16 row pixels of a block are called vectors. Computation is performed block by block in raster manner. The centre vector of a block is called pivot vector. Each block produces the output of $s \times 16$ pixels and written to the output image. The organization of an image for the vectorized algorithm using SE of size 5×1 is shown in Figure 5.8. The 2-D dilation operation is performed by applying 1-D vectorized dilation on columns. Then resultant image data is reorganized for fast loading of vectors. Finally, 1-D dilation operation is carried out again on columns of the resultant image to complete 2-D dilation operation. For 2-D erosion operation, substitute min for max. The gray-scale opening and closing operations can be defined as sequence of erosion and dilation and vice versa.

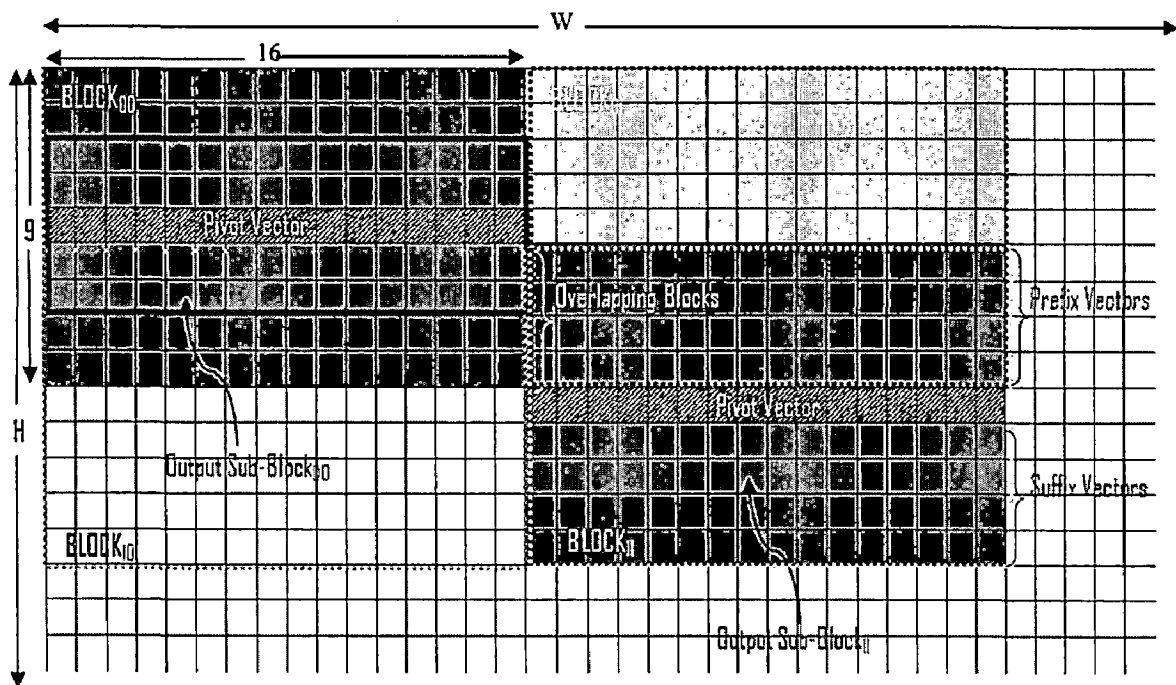


Figure 5.8: Organization of Image for Vectorized Gray-Scale Morphological Processing Using SE of size 5x1

5.3.2 VECTORIZED ALGORITHM

Let A_0 and O_0 are the addresses of the first pixel of the input and the output image respectively. Let C_i is the Base Address of the Pivot Vector for row i and C_o is the Address of the Pivot Vector for Block j . Let, $VR_0, \dots, VR_4, VS_1, \dots, VS_4, VT_1, \dots, VT_3$ and V_{TEMP} are vectors with element size of 16 each. Let N_w is the number of overlapping windows, each of size $2s-1$ where s is the size of SE. Pseudo code of the vectorized algorithm for gray-scale morphological dilation is given below.

Input: IN is an HxW Input Image

Output: OUT is an HxW Filtered Image

For i=0 to N_w

$C_i = W*4 + (W*5)*i$;

/ Step 1: Generating Overlapping Blocks */*

For j=0 to B_v

$C_o = C_i + 16*j$;

/ Step 2 (a): Load and Compare Prefix Vectors */*

$VR_0 = \text{load IN}[A_0 + C_o]$; */* Load pivot vector VR_0 */*

$V_{TEMP} = \text{load IN}[A_0 + C_o - W]$;

$VR_1 = \max(VR_0, V_{TEMP})$; */* Max of VR_0 and V_{TEMP} */*

$V_{TEMP} = \text{load IN}[A_0 + C_o - W*2]$;

$VR_2 = \max(VR_1, V_{TEMP})$;

$V_{TEMP} = \text{load IN}[A_0 + C_o - W*3]$;

$VR_3 = \max(VR_2, V_{TEMP})$;

$V_{TEMP} = \text{load IN}[A_0 + C_o - W*4]$;

$VR_4 = \max(VR_3, V_{TEMP})$;

/ Step 2 (b): Load and Compare Suffix Vectors */*

$V_{TEMP} = \text{load IN}[A_0 + C_o + W]$;

$VS_1 = \max(VR_0, V_{TEMP})$;

$V_{TEMP} = \text{load IN}[A_0 + C_o + W*2]$;

$VS_2 = \max(VS_1, V_{TEMP})$;

$V_{TEMP} = \text{load IN}[A_0 + C_o + W*3]$;

$VS_3 = \max(VS_2, V_{TEMP})$;

$V_{TEMP} = \text{load IN}[A_0 + C_o + W*4]$;

$VS_4 = \max(VS_3, V_{TEMP})$;

/ Step 3: Merging Step */*

$VT_1 = \max(VR_1, VS_3)$;

$VT_2 = \max(VR_2, VS_2)$;

$VT_3 = \max(VR_3, VS_1)$;

/ Step 4: Writing Result */*

$OUT[O_0 + C_o - W*2] = \text{store}(VR_4)$;

$OUT[O_0 + C_o - W] = \text{store}(VT_3)$;

$OUT[O_0 + C_o] = \text{store}(VT_2)$;

$OUT[O_0 + C_o + W] = \text{store}(VT_1)$;

$OUT[O_0 + C_o + W*2] = \text{store}(VS_4)$;

End

End

5.3.3 RUN-TIME PERFORMANCE

The vectorized algorithm was run over SVME-183 board. The SVME-183 is an embedded Single Board Computer (SBC) board as shown in Figure 5.2. It is housed in a VME 64x chassis. The card has MPC7447A PowerPC (AltiVec Technology) 1.2 GHz, each with 512 MB of SDRAM. The SVME-183 SBC is supported by Wind River's VxWorks real-time operating system (RTOS). Run-time for various HARDWARE implementations is given in Table 5.1.

TABLE 5.1: RUN-TIME FOR HARDWARE IMPLEMENTATIONS OF MORPHOLOGICAL PRE-PROCESSING ALGORITHM

| S. No. | SE Size | Dilation or Erosion Time (in milliseconds) | | |
|--------|---------|---|-------|------|
| | | (1) | (2) | (3) |
| 1. | 3x3 | 33.33 | 16.67 | 3.33 |
| 2. | 5x5 | 116.67 | 16.67 | 3.33 |
| 3. | 7x7 | 200.00 | 16.67 | 3.33 |
| 4. | 9x9 | 333.33 | 16.67 | 3.33 |
| 5. | 11x11 | 500.00 | 16.67 | 3.33 |
| 6. | 13x13 | 666.67 | 16.67 | 3.33 |
| 7. | 15x15 | 883.33 | 16.67 | 3.33 |
| 8. | 17x17 | 1150.00 | 16.67 | 3.33 |
| 9. | 19x19 | 1416.67 | 16.67 | 3.33 |
| 10. | 21x21 | 1716.67 | 16.67 | 3.33 |

(1) Naïve 2-D Implementation

(2) Scalar Constant-Time Gray-Scale Morphological Processing Algorithm

(3) Vectorized Constant-Time Morphological Processing Algorithm

*Image Size: 320x240 Pixels

5.4 REAL-TIME IMPLEMENTATION OF ROBUST LONG RANGE TARGET DETECTION ALGORITHM

In addition to pre-processing module, some other modules also had scope of vectorization. The selected modules of detection algorithm those have also been vectorized are followings.

- Variance Calculation Module
- Difference Image Generation Module
- Thresholding Module

5.5 REAL-TIME VIDEO CAPTURE, DISPLAY AND OVERLAYING MODULE

Real-time video capture, display and overlaying module is developed to capture real-time video, display on the directly connected display unit. The symbologies for the detection are generated with the help of X11 graphics programming. The developed module uses PMC 704 hardware abstracted library to manipulate and access video data produced by the PMC 704. The output of the developed real-time video display/overlay module is shown in Figure 5.9. The library allows the application to:

- Controls PMC from API
- Modify the Hue, Saturation, Brightness and Contrast of the Images Being Captured
- Real-Time Start and Stop Capture of Frames
- Specify a Specific Number of Frames to be Captured
- Set and Get the Video Input Mode
- Set and Get the Video Resolution
- Real-Time Application Callback Function Triggered at End of Field/Frame
- Count the Number of Frames Captured

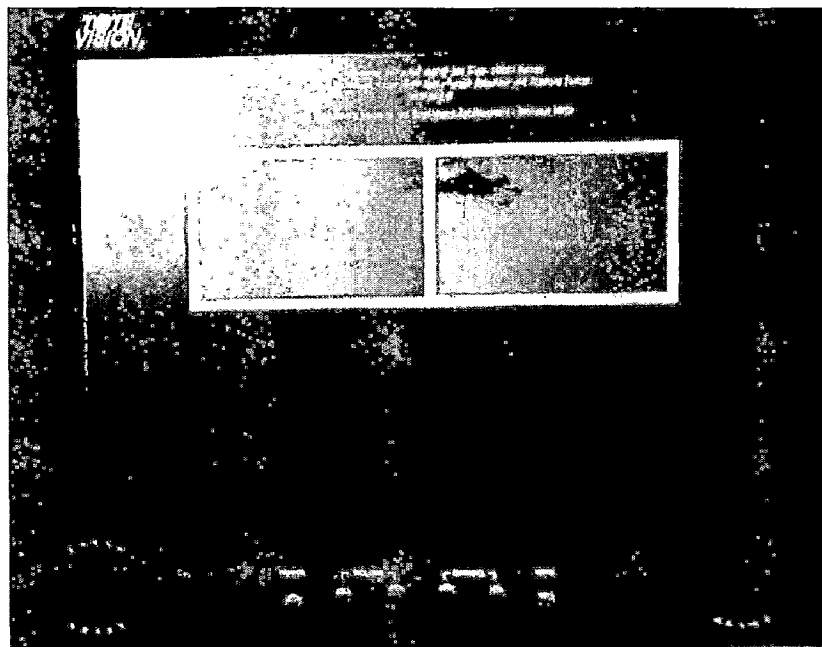


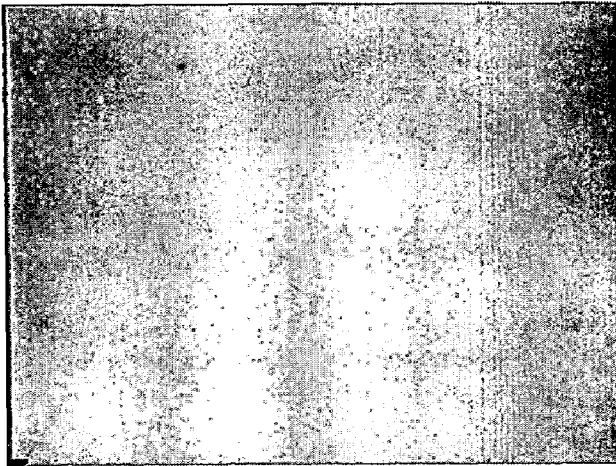
Figure 5.9: Snapshot of Display/ Overlaying Output

The real-time video capture, display and overlaying module has been developed as a part of real-time implementation of proposed robust long range target detection algorithm on hardware and has following functionalities.

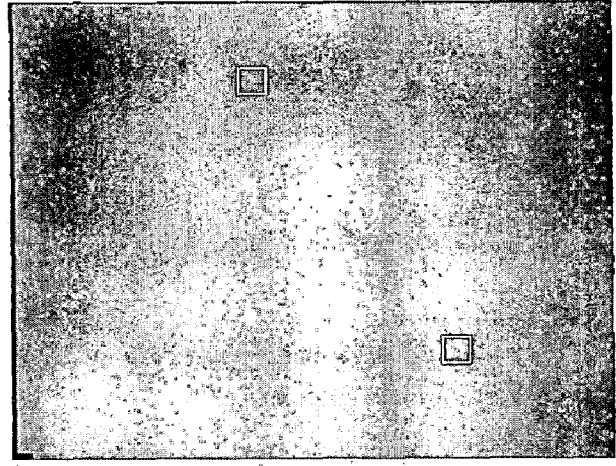
- Real Time Frame Capture
- Resizing of Frames (640x480 Pixels to 320x240 Pixels)
- Display of Startup/Bootup Message
- Division of Screen to Display Input as well as Output (Detected) Video
- Generation of Window around the Detected Positions of Targets and Overlaying on Detected Image Frame
- Generation and Overlaying of Position (Coordinates) and Size of Targets
- Highlighting of Approaching Targets

5.6 HARDWARE IMPLEMENTATION RESULTS

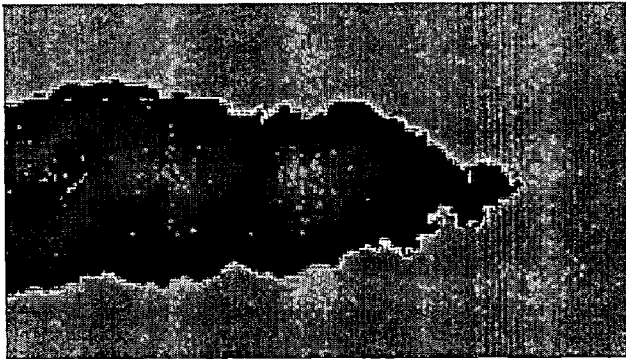
The detection performance of proposed long range target detection algorithm has also been tested on PowerPC hardware implementation. In all cases, the detection performance has been found same as the simulated performance which is obvious. Sample hardware implementation results are shown in Figure 5.10.



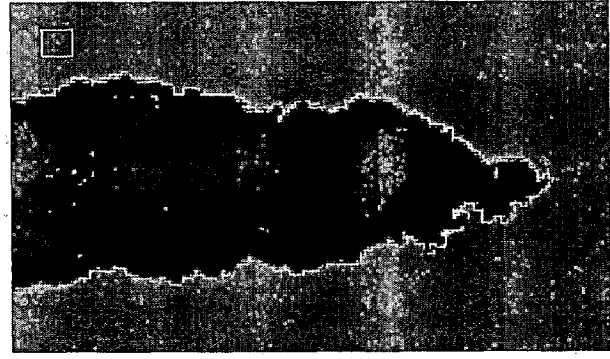
(1-a)



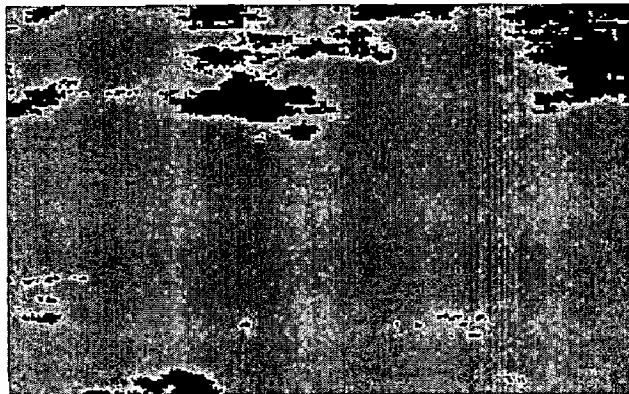
(1-b)



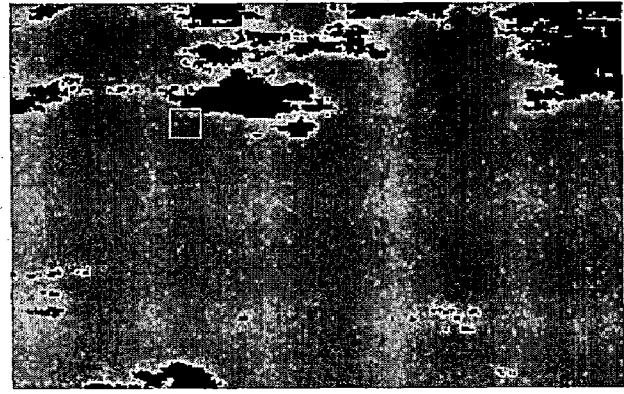
(2-a)



(2-b)



(3-a)



(3-b)

Figure 5.10: Hardware Implementation Results (1-a), (2-a) and (3-a) are Input Frames of Image Sequence 1, 3 and 5 respectively, (1-b), (2-b) and (3-b) are Detection Results of Proposed Robust Target Detection Algorithm

5.7 LABORATORY PROTOTYPE AND EXPERIMENTAL SETUP

The proposed robust long range target detection algorithm is implemented on SVM 183 PowerPC board. The real-time performance of 25 frames/ sec has been achieved with a single PowerPC 7447 (AltiVec) processor. The components and actual laboratory prototype of the hardware implementation of proposed robust long range range target detection algorithm are shown in Figure 5.11 and 5.12 respectively.

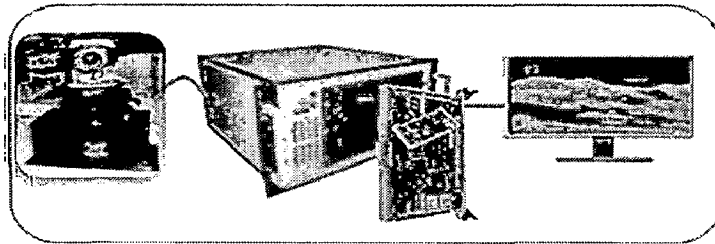


Figure 5.11: Components of Hardware Implementation of Proposed Robust Long Range Target Detection Algorithm

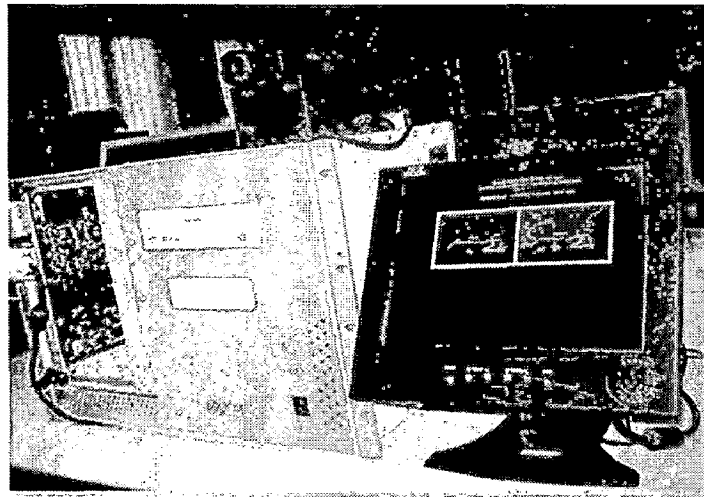


Figure 5.12: Laboratory Prototype for Real-Time Hardware Implementation of Proposed Robust Long Range Target Detection Algorithm

6 CONCLUSION AND FUTURE SCOPE

This dissertation report introduces the novel Adaptive Selective Double Structuring element Top-Hat Transform (Adapt-Sel-DSTHT) based robust point and small target detection algorithm for visible and infrared image sequences. The novel Adapt-Sel-DSTHT filter predicts the background better than the existing pre-processing filters. Results show consistent performance for different kinds of possible scenario with high probability of detection and very low probability of false alarm. The proposed Adapt-Sel-DSTHT based robust long range target detection algorithm has also been implemented on PowerPC hardware with real-time processing capability.

Fusion of visible and infra-red image frames could be taken as future work to further enhance the probability of detection and to reduce the false alarms.

RESEARCH PUBLICATIONS AND AWARD

1. Ram Saran, Anil K. Sarje, "Vectorization of Constant-Time Gray-Scale Morphological Processing Algorithm Using Altivec Technology," Proc. IEEE Conference on Communications 2011, India, 28-30 Jan 2011, pp. 1-5.
2. Ram Saran, Anil K. Sarje, H B Srivastava, "Robust Point and Small Target Detection Algorithm Based on Selective-Contour Structuring Element Morphology," IET (Formerly IEE) Journal Electronics Letters, Communicated on 25 Jan 2011.
3. Ram Saran, Anil K. Sarje, "LRT-DetSim: Long-Range Airborne Target Detection Simulator for Infra-Red Image Sequences" Defence Science Journal, Communicated on 28 Oct 2010.
4. Ram Saran, Anil K. Sarje, "Robust Long Range Target Detection Algorithm Using Adaptive Selective Top-Hat Transform," IEEE International Conference of Image Information Processing 2011, Shimla, India, Communicated on 1 Jun 2011.
5. Ram Saran, "ALoRT-DetSys: Advanced Long-Range Airborne Target Detection System for Visible and Infra-Red Image Sequences" Proc. Computer Society of India (CSI) National Students' Convention 2011, India, 12 Mar 2011, pp. 34-38.

AWARD

CSI National Students' Convention NSC-2011: National Level Paper/Project Competition, Bharati Vidyapeeth University, New Delhi, 12 March 2011.

- First Position (Best Project Award)

REFERENCES

- [1] Boyd Cook "PIRATE the IRST for Eurofighter TYPHOON," *Infrared Technology and Applications XXVIII*, Proc. SPIE, vol. 4820, pp. 897-907, 2003.
- [2] Hari Babu Srivastava, Y B Limbu, Ram Saran, Ashok Kumar, "Airborne Infrared Search and Track Systems," *Defence Science Journal*, Vol. 57, No. 5, pp.739-753, September 2007.
- [3] Charlene E. Cafer, Jerry Silverman, Steven DiSalvo, Richard W. Taylor, "Post processing of point target detection sinusoidal filters," *Signal and Data Processing of Small Targets*, Proc. SPIE, Vol. 4048, pp. 104-110, 2000.
- [4] Ram Saran, Hari Babu Srivastava, Ashok Kumar, " Encountering False Alarms for Detection of Point Targets in Highly Cluttered Background," *Photonics Europe 2008*, Cardiff, Wales, United Kingdom, Proc. SPIE, Vol. 7114, pp. 71140N-1-71140N-8, 2008.
- [5] Suyog D. Deshpande, Meng H. Er, Ronda Venkateswarlu, "Max-mean and max-median filters for detection of small targets," *Signal and Data Processing of Small Targets*, Proc. SPIE, vol. 3809, pp. 74-83, 1999.
- [6] Nengli Dong, Gang Jin, Bo Qi, and Jiaguang Ma, "New approach to detect dim moving point targets based on motion analysis," *Signal and Data Processing of Small Targets*, Proc. SPIE, Vol. 4473, pp. 34-42, 2001.
- [7] Jian-Nan Chi, Ping Fu, Dong-Shu Wang, Xin-In-He Xu, "A Detection Method of Infra-red Image Small Image Target Based on Order Morphology Transformation and Image Entropy Difference," *Fourth International Conference on Machine Learning and Cybernetics*, Guangzhou, China, 18-21 August, Proc. IEEE, vol.1, pp. 5111-5116, 2005.
- [8] Xinyu Wang, Jingdong Chen, Huosheng Xu and Xi Chen, "Adaptive Method for Infrared Small Target Detection Based on Gray-Scale Morphology and Backward Cumulative Histogram Analysis," *International Conference on Information and Automation*, Zhuhai/Macau, China, June 22 -25, Proc. IEEE, vol. 1, pp. 173-177, 2009.
- [9] Jiefeng Guo, Guilin Chen, "Analysis of selection of structural element in mathematical morphology with application to infrared point target detection," *Infrared Materials, Devices, and Applications*, Proc. SPIE, Vol. 6835, pp. 68350P-68356P, 2007.

-
- [10] Xiangzhi, Bai, Fugen, Zhou, Yongchun, Xie, Ting, Jin, "Modified Top-hat transformation Based on Contour Structuring Element to Detect Infrared Small Target," 3rd IEEE Conference on Industrial Electronics and Applications, Singapore, 3-5 June, Proc. IEEE, pp. 575-579, 2008.
- [11] S. Kim, Y. Yang and J. Lee, "Robust detection of horizontal small targets using synergistic spatial filtering," IEEE Electronics Letters, vol. 45, no.12, June 4, 2009.
- [12] Gary Hower, Wei Kuo, Charles Kenney and Grant Hanson and, Jim Bobinchak, "Detection of Small IR Objects Using Wavelets, Matched Subspace Detectors, and Registration," Signal and Data Processing of Small Targets, Proc. SPIE, vol. 4728, pp. 12-23, 2002.
- [13] Mukesh A. Zaveri, Anant Malewar, S. N. Merchant, and Uday B. Desai, "Wavelet based Detection and Modified Pipeline Algorithm for Multiple Point Targets in InfraRed image sequences," ICVGIP, Kolkata, 2002.
- [14] Wang Ting, Shenyuan Yang, "Weak and Small Infrared Target Automatic Detection Based on Wavelet Transform," Second International Symposium on Intelligent Information Technology Application, China, Proc. IEEE, pp. 697-701, 2008.
- [15] Hari Babu Srivastava, Ram Saran, Ashok Kumar, "Modified motion-based algorithm for detection of dim point targets in IR image sequences," Optical Sensing II, Proc. SPIE, vol. 6189, pp. 61891M1-61891M12, 2006.
- [16] Xiangzhi Bai, Fugen Zhou, Yongchun Xie, Ting Jin, "Adaptive Morphological Method for Clutter Elimination to Enhance and Detect Infrared Small Target," Proc. IEEE, International Conference on Internet Computing in Science and Engineering, pp. 28-33, 2008.
- [17] Feng-Yun Zhu, Shi-Yin Qin, "A Detection Algorithm for Manoeuvring IR Point Target and Its Performance Evaluation," 2nd IEEE/ASME International Conference on Mechatronic and Embedded Systems and Applications, Beijing, Proc. IEEE, pp. 1-5, August 2007.
- [18] Kai Wang, Yan Liu, Xiaowei Sun, "Small Moving Infrared Target Detection Algorithm under Low SNR Background," Fifth International Conference on Information Assurance and Security, China, Proc. IEEE pp.95-97, 2009.

-
- [19] Xiaoqing Luo, "A Novel Fusion Detection Algorithm for Infrared Small Targets," Third International Symposium on Intelligent Information Technology Application, Proc. IEEE, pp.427-430, 2009.
- [20] Gary Hower, Wei Kuo, Charles Kenney and Grant Hanson and, Jim Bobinchak, "Detection of Small IR Objects Using Wavelets, Matched Subspace Detectors, and Registration," Signal and Data Processing of Small Targets, Proc. SPIE, Vol. 4728, pp. 12-23, 2002.
- [21] Wang Ting, Shenyuan Yang, "Weak and Small Infrared Target Automatic Detection Based on Wavelet Transform," Second International Symposium on Intelligent Information Technology Application, China, Proc. IEEE, pp. 697-701, 2008.
- [22] Feng-Yang Hsieh, Chin Chauan Han, Nai-Shen Wu, and Kuo-Chin Fan, "A novel approach to noise removal and detection of small objects with low contrast," Signal Processing, ACM, Vol. 86 , Issue 1, pp. 71-83, January, 2006.
- [23] Young Yu, Lei Guo, "Infrared Small Moving Target Detection Using Facet Model and Particle Filter," Congress on Image and Signal Processing, Proc. IEEE, pp. 206-210, 2008.
- [24] Zhenhua Wei, Yanping Liu, "Research on Small Object Detection and Tracking Based on Particle Filter," Second International Conference on Intelligent Computation Technology and Automation, Proc. IEEE, pp. 403-406, 2009.
- [25] Yen, J., Chang, F., and Chang, S., 'A New Criterion for Automatic Multilevel Thresholding', IEEE Transaction on Image Processing, Vol. 4, No. 3, pp. 370-378, 1995.
- [26] "Matlab 7 Programming Fundamentals: Users' Manual", Matlab 7.5, September 2007.
- [27] "Matlab 7 Creating Graphical User Interfaces", Matlab 7.5, September 2007.
- [28] Susan Seale, "PowerPC G4 Architecture White Paper: Delivering Performance Enhancement in 60x Bus Mode," in Motorola Digital DNA, 2000. [Online]. Available: cache.freescale.com/files/product/doc/G4WP.pdf
- [29] Diefendorff K, Dubey P K, Hochsprung R, and Scale H, "Altivec extension to PowerPC accelerates media processing," IEEE Micro, vol.20, no. 2, pp.85-95, Mar-Apr 2000.

-
- [30] Software User's Manual, SVME/DMV-183, VxWorks 6.3 BSP & Driver Suite, Curtiss-Wright Controls Embedded Computing, Ontario, Canada, Document Number 814646, Version 4, April 2007.
- [31] "SVME/DMV-183 Product Data Sheet," Curtiss-Wright Controls Embedded Computing, www.cwcembedded.com, last accessed on 25 Oct 2010.
- [32] "PMC-704 Product Data Sheet," Curtiss-Wright Controls Embedded Computing, www.cwcembedded.com, last accessed on 25 Oct 2010.